[AMERICAN JOURNAL OF SCIENCE, VOL. 293, SUMMER, 1993, P. 671–721]

GEOCHEMISTRY AND ORIGIN OF VOLCANICS IN THE ORDOVICIAN PARTRIDGE FORMATION, BRONSON HILL ANTICLINORIUM, WEST-CENTRAL MASSACHUSETTS

KURT HOLLOCHER
Geology Department, Union College, Schenectady, New York 12308

ABSTRACT. The Partridge Formation is largely composed of aluminous sulfidic mica schist but contains substantial quantities of metamorphosed bimodal mafic and felsic volcanics chemically similar to the underlying Ammonoosuc Volcanics. The volcanics in the Partridge Formation were regionally metamorphosed in the kyanite + muscovite + staurolite through sillimanite + orthoclase zones during the Devonian Acadian Orogeny. The mafic Partridge volcanics, now amphibolites, have compositions similar to low-K tholeiitic basalts. The amphibolites generally have straight REE patterns, are slightly LREE-enriched, have small positive Eu anomalies, and all have negative Nb anomalies. Modeling indicates that the basaltic protoliths to the amphibolites were derived from 3 to 15 percent partial melting of a spinel lherzolite mantle source having flat chondritic abundances for most elements, but depleted by about 1.6x for Hf and Zr for most samples, and depleted in Nb by about 3x for all samples. The primary magmas were modified by low pressure fractional crystallization of olivine and possibly also of pyroxene and plagioclase. The felsic Partridge volcanics, now gneisses, have calc-alkaline compositions ranging from dacite to rhyolite. The felsic gneisses have somewhat LREE-enriched patterns and negative Nb, Sr, Eu, and Ti anomalies. Modeling indicates that the felsic gneisses were derived from the partial melting of a pyroxene + plagioclase + olivine granulite source having a Nb-depleted composition similar to that of the Partridge amphibolites. Melting presumably took place in the deep crust. Although identification of the tectonic environment for eruption of the Partridge volcanics is somewhat problematic, evidence favors a back-arc basin setting. The volcanics in the Partridge Formation, and by analogy the Ammonoosuc Volcanics, record an episode of Taconian igneous activity that is chronologically similar to but in some respects lithologically and chemically different from the presumed main part of the Taconian magmatic island arc exposed as calc-alkaline dome gneisses in the Bronson Hill anticlinorium. A back-arc basin setting for the Ordovician volcanics requires that they be in fault contact with the underlying dome gneisses.

INTRODUCTION

In middle to late Ordovician time an island arc lay to the east of the North American continent (present coordinates). As the intervening ocean basin closed, volcanic and plutonic rocks were emplaced in the island arc, and flysch was deposited westward into the marine forearc trench. Collision of the arc with North America produced extensive Taconian deformation and regional metamorphism up to sillimanite grade in the accretionary prism and in portions of involved North American basement (Robinson and Hall, 1980; Hall and Robinson, 1982;

Stanley and Ratcliffe, 1985). Local evidence of high-pressure metamorphism is also preserved (Laird and Albee, 1981).

There are two principal igneous components of the Taconian island arc. The first includes the Ammonoosuc Volcanics and volcanics in the overlying Partridge Formation (fig. 1). A concordant zircon U/Pb age of 453 ± 2 my has been determined on a metamorphosed felsic volcanic from the upper member of the Ammonoosuc, and a zircon U/Pb age of

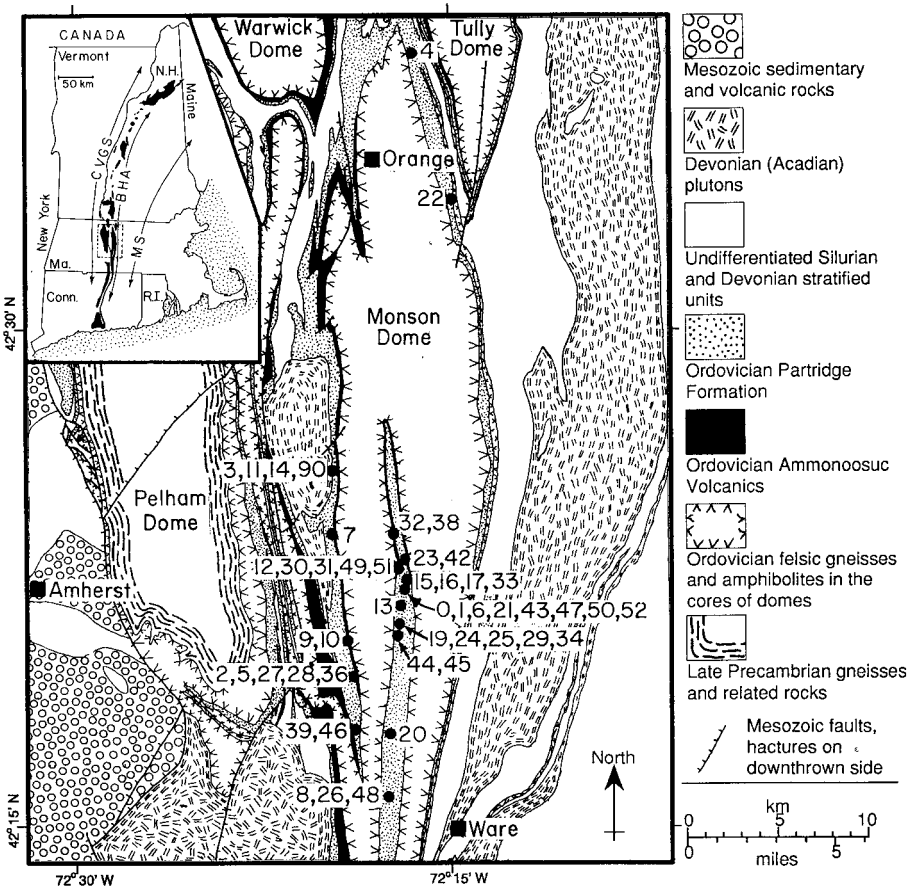

Fig. 1. Simplified geologic map of west-central Massachusetts showing sample locations. Geology is after Zen (1983), except that areas of Partridge Formation to the east of the Bronson Hill anticlinorium and in the Amherst area are shown as undifferentiated Silurian and Devonian units (Peter Robinson, written communication, 1992; in part Robinson and others, 1989). Inset map is of southern New England showing the locations of the Connecticut Valley-Gaspé synclinorium (CVGS), the Merrimack synclinorium (MS), and the Bronson Hill anticlinorium (BHA). In the Bronson Hill anticlinorium the areas of coarse-grained dome gneisses occupying the cores of Acadian structural domes are shown in black (after Field, ms).

449 +3/−2 my has been determined on a metamorphosed felsic volcanic having relict pyroclastic textures from near the base of the Partridge Formation (Tucker and Robinson, 1990). The second igneous component of the arc includes generally coarse-grained gneisses of probable plutonic origin that structurally underlie the Ammonoosuc Volcanics. These rocks are mainly tonalitic through granitic gneisses with minor quantities of mafic and ultramafic rock that are now exposed in a series of Acadian (Devonian) structural domes in the Bronson Hill anticlinorium (fig. 1). These rocks will be referred to here as dome gneisses. The dome gneisses belong to the Oliverian magma series of Billings (1937) and are generally thought to be the plutonic roots of the Taconian island arc. Felsic dome gneisses have yielded zircon U/Pb ages of 454 to 442 ± 3 my (Tucker and Robinson, 1990), a range that includes the zircon ages from the Ammonoosuc Volcanics and Partridge Formation. The Pelham dome (fig. 1) also contains rocks of late Proterozoic age, which are not part of the following discussion. Although the Taconian plutonic and volcanic rocks are not known to have been metamorphosed during the Ordovician, they were deformed and metamorphosed during the Acadian Orogeny. Metamorphism in the study area ranged from the kyanite + staurolite + muscovite zone to the sillimanite + orthoclase zone (Tracy, Robinson, and Thompson, 1976).

The Taconian volcanics and the underlying dome gneisses have been studied in some detail, but many questions remain as to their origin as igneous rocks and their structural and petrologic relationships to each other and to Taconian tectonics. This paper attempts to answer some of these questions by providing a better understanding of the geochemical characteristics and origins of the Ammonoosuc Volcanics and volcanics in the Partridge Formation as part of Taconian igneous activity in the central Bronson Hill anticlinorium. This will allow a better understanding of the petrologic development of the Taconian island arc system and aid the development of more accurate tectonic models of eastern North America during Ordovician time. An improved understanding of the pre-Acadian structural and stratigraphic relationships among the Taconian rocks will also help unravel the structural development of west-central New England during the Devonian Acadian Orogeny.

LITHOLOGY

The Ammonoosuc Volcanics form the basal unit in the stratified Paleozoic sequence in the Bronson Hill anticlinorium. The Ammonoosuc is up to 1200 m thick and has a well defined internal stratigraphy (Schumacher, 1988): a lower mafic member containing generally minor amounts of felsic rocks and a laterally extensive calcareous horizon, a middle member of fine-grained pink garnet quartzite (coticule), and an upper felsic member containing minor amounts of mafic rocks. Relict volcanoclastic textures and pillow lavas have been described (Schumacher, 1988). Field, petrologic, and whole rock geochemical evidence indicates that the Ammonoosuc Volcanics are compositionally bimodal (fig.

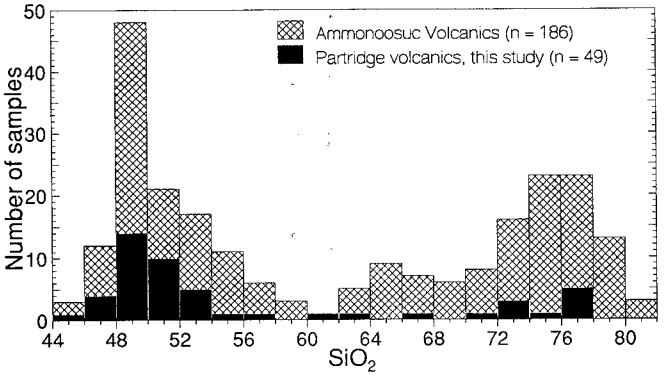

Fig. 2. Histogram showing the abundance of analyzed samples from the Ammonoosuc Volcanics and volcanics in the Partridge Formation with respect to SiO_2 content. Ammonoosuc analyses are from Aleinikoff (1977), Schumacher (ms), Leo, Zartman, and Brookins (1984), Shumway (ms), and Leo (1985, 1991). Partridge analyses are from this paper. These sources of data are used throughout this paper.

2; Aleinikoff, 1977; Schumacher, ms and 1988; Shumway, ms; Leo, Zartman, and Brookins, 1984; Leo, 1985, 1991).

The Partridge Formation overlies the Ammonoosuc Volcanics along a contact defined in Massachusetts by the first appearance of sulfidic mica schist. The Partridge Formation is largely composed of aluminous pyrrhotite-mica schist but also contains interbedded metamorphosed bimodal volcanics (fig. 2) about 150 m thick. Minor amounts of calc-silicate rock and coticule also occur. Some amphibolites with graded layering have been interpreted as layered mafic tuffs or submarine mafic debris flows (Hollocher, ms). Volcanoclastic textures are preserved in rocks metamorphosed in the chlorite and biotite zones in the Bernardston area, west of the Warwick dome (David Elbert, oral communication, 1989). Except for Hollocher (ms) and work on some small ultramafic bodies in this unit (Wolff, ms; Tracy, Robinson, and Wolff, 1984), little work has been done on volcanics in the Partridge Formation.

Direct comparison (figs. 2, 3, 4, 5, 6, 7, 12, 14, 15) and cluster and discriminant analysis (not shown) for the mafic and felsic rocks used in this study (see caption of fig. 2) show that the chemical compositions of the Ammonoosuc and Partridge volcanics are similar, and no reliable discriminant has been found. The two sets of volcanics are considered here to be part of the same volcanic series because of their chemical and lithologic similarity, similarity in age, and the stratigraphic succession of the Ammonoosuc Volcanics by the Partridge Formation.

PETROLOGY OF THE ANALYZED SAMPLES

Forty nine samples of metamorphosed igneous rocks were collected from the Partridge Formation: 35 amphibolites, 4 intermediate gneisses,

and 10 felsic gneisses (fig. 1). Samples were collected from massive, homogeneous layers and were taken as far as possible from veins, pegmatites, calc-silicate rocks, texturally inhomogeneous areas, sulfidic zones, biotite-rich reaction zones, and other potential indications of contamination of the volcanic layers. Although amphibolites make up 80 to 90 percent of exposures of volcanics in the Partridge Formation, they make up only 65 percent of the analyzed samples since felsic and intermediate gneisses were sampled preferentially. The amphibolite samples are, however, representative of the exposed massive amphibolites. Chemical analyses of these rocks are given in table 1, and norms and modes are given in table 2.

The 35 analyzed Partridge amphibolites span an SiO_2 range of 45.33 to 54.56 percent, nominally corresponding to basalt and basaltic andesite. These rocks have assemblages of hornblende + plagioclase ± quartz ± biotite ± garnet ± cummingtonite ± gedrite ± orthopyroxene ± ilmenite ± magnetite ± sphene ± pistacite (see Hollocher, 1991, for a discussion of phase relations).

The four analyzed Partridge intermediate gneisses span an SiO_2 range of 57.05 to 67.53 percent, nominally corresponding to andesite and dacite. These rocks are plagioclase + quartz + biotite gneisses ± hornblende ± garnet ± K-feldspar ± ilmenite ± magnetite ± cummingtonite. They vary highly in composition and cannot be related to one another or to the Partridge mafic or felsic rocks by simple geochemical processes. Although some of the intermediate gneisses may have igneous protoliths and nearly original igneous compositions, there is no internally consistent way to demonstrate this, so these rocks are not discussed further here.

The ten analyzed Partridge felsic gneisses span an SiO_2 range of 71.59 to 77.49 percent, in the nominal range of rhyodacite and rhyolite. These rocks are mineralogically and texturally similar to one another, in contrast to the diverse intermediate gneisses. The felsic gneisses contain the assemblages quartz + plagioclase + biotite ± K-feldspar ± garnet ± ilmenite ± magnetite ± muscovite. Sample 45 has minor sillimanite and staurolite.

PROTOLITHS AND PRE- AND SYNMETAMORPHIC ALTERATION

Major-element analyses and norms calculated from them can be used to identify the igneous protoliths of metamorphosed igneous rocks either by direct comparison or by using igneous rock classification schemes (Streckeisen, 1967). Many of the major elements, including Si, Mg, Ca, Na, and K, are known to be mobile during various chemical alteration processes, making suspect the conclusions drawn from them. Some trace elements, such as Nb, Y, Zr, and Ti, tend to be much less mobile during most alteration processes. These elements have also been shown to vary systematically with igneous rock type and so can be used to classify the igneous protoliths of metamorphic rocks while avoiding problems associated with the mobile major elements (fig. 3). Despite

TABLE 1

Major and trace element analyses of the Partridge Formation volcanics

	Amphibolites															
SAMPLE	0	1	2A	3A	90	4	5A	6	7	8A	9	10	11	12A	13A	14A
SiO2	45.33	46.40	46.92	46.95	47.61	48.18	48.34	48.36	48.40	48.56	49.23	49.26	49.28	49.35	49.42	49.45
TiO2	0.56	0.88	1.00	0.62	0.65	1.36	0.88	1.34	0.80	1.42	0.56	0.86	0.72	1.55	0.95	2.37
Al2O3	14.56	16.79	16.19	17.99	18.81	15.34	16.18	16.39	16.08	15.16	17.58	15.94	16.50	16.15	16.94	15.53
Fe2O3	12.23	2.00	1.26	1.13	9.66	2.83	1.19	4.40	1.47	1.03	1.34	1.42	1.17	1.68	3.78	1.62
FeO	**	9.01	10.91	8.15	**	8.84	8.07	9.60	7.97	10.72	7.55	8.90	7.55	12.37	6.60	10.65
MnO	0.19	0.21	0.17	0.15	0.16	0.16	0.16	0.13	0.15	0.18	0.14	0.17	0.16	0.14	0.16	0.20
MgO	15.17	10.14	7.55	10.72	9.56	11.02	10.29	6.08	9.93	10.22	8.39	9.40	9.01	6.81	6.73	6.38
CaO	10.05	11.69	13.11	12.12	11.71	8.93	11.53	9.79	12.18	9.01	11.51	10.47	11.79	4.78	14.03	10.02
Na2O	1.49	1.90	1.64	1.48	1.66	2.42	2.09	2.76	1.93	2.01	2.65	2.18	2.60	3.53	1.08	2.98
K2O	0.19	0.31	0.33	0.21	0.14	0.13	0.71	0.55	0.22	1.10	0.29	0.30	0.29	3.03	0.28	0.16
P2O5	0.07	0.10	0.11	0.07	0.07	0.14	0.07	0.12	0.07	0.18	0.08	0.10	0.08	0.17	0.13	0.27
Total	99.84	99.43	99.19	99.59	100.03	99.35	99.51	99.52	99.20	99.59	99.32	99.00	99.15	99.56	100.10	99.63
Mg/(Mg+Fet)	0.71	0.63	0.53	0.68	0.66	0.63	0.67	0.44	0.66	0.61	0.63	0.62	0.65	0.47	0.55	0.48
Ca/(Ca+Na)	0.79	0.77	0.82	0.82	0.80	0.67	0.75	0.66	0.78	0.71	0.71	0.73	0.71	0.43	0.88	0.65
Trace Elements in ppm																
V	183	282	373	194	195	360	240	472	237	312	185	279	246	272	355	286
Cr	759	440	205	274	242	195	414	3	424	278	306	405	548	260	172	221
Ni	296	150	72	198	159	80	169	12	150	148	99	151	96	85	30	86
Zn	82	92	95	75	71	103	63	135	69	84	63	87	71	96	77	123
Ga		16	18	14		19	15	20	15	18	15	16	15	18	17	21
Rb		9	7	7		1	13	8	2	42	2	8	4	75	5	2
Sr	79	162	196	149	173	151	152	239	138	166	187	249	191	146	166	379
Y		15	14	11		27	20	27	17	26	11	18	13	30	14	44
Zr	27	40	40	32	30	60	30	46	35	85	27	41	27	88	31	202
Nb	1.6	1.9	2.9	0.9	1.1	1.4	0.9	0.8	0.3	1.7	1.6	0.5	1.1	3.3	1.3	4.8
Ba	6	51	222	27	48	18	2145	34	88	707	117	100	115	100	366	8

La	3.1	4.7	3	3.0		5	1	4.7	1.6	7.4	3.6	3.8	3.2	7.4	8	11.8
Ce	8.1	12.0	12	7.7	10	17		12.0	5.4	17.6	8.2	11.4	7.8	19.2	11	29.1
Pr	1.06	1.60		1.03				1.71	0.88	2.44	1.11	1.63	1.18	2.82		4.24
Nd	5.1	7.7		5.1				9.1	5.1	12.1	5.4	7.9	5.7	14.1		20.9
Sm	1.45	2.15		1.49				3.09	1.84	3.65	1.55	2.36	1.80	4.23		5.82
Eu	0.58	0.81		0.66				1.18	0.77	1.32	0.62	0.87	0.72	1.38		1.88
Gd	1.58	2.31		1.76				3.97	2.37	4.25	1.79	2.85	2.14	4.63		6.46
Tb	0.27	0.42		0.31				0.74	0.48	0.75	0.31	0.50	0.37	0.84		1.16
Dy	1.72	2.73		2.00				4.79	3.05	4.84	2.10	3.26	2.48	5.51		7.47
Ho	0.38	0.58		0.43				1.06	0.66	1.02	0.46	0.71	0.52	1.15		1.58
Er	1.07	1.61		1.23				3.10	1.89	2.88	1.30	2.04	1.46	3.21		4.35
Tm	0.15	0.23		0.18				0.46	0.26	0.42	0.19	0.29	0.20	0.48		0.64
Yb	1.01	1.56		1.16				2.95	1.71	2.68	1.26	1.99	1.40	2.97		4.04
Lu	0.16	0.23		0.18				0.46	0.26	0.42	0.20	0.30	0.22	0.46		0.60
Hf	0.72	1.25		0.88				1.87	1.30	2.60	0.78	1.37	0.95			
Pb		5	6	4		6	7	6	4	7	4	8	4	6	1	13
Th	0.70	0.86	3	0.51		1	0	0.27	0.24	0.76	0.76	0.94	0.59	0.29	2	1.21
U	0.17	0.20		0.15				0.47	0.09	0.30	0.20	0.22	0.15	0.06		0.27
Cen/Ybn	2.1	2.0		1.7				1.1	0.8	1.7	1.7	1.5	1.4	1.7		1.9
Eun/Eu*	1.17	1.11		1.24				1.03	1.13	1.03	1.14	1.03	1.13	0.95		0.94

Analytical methods are given in app. 1.

* Ratio of the chondrite-normalized Eu concentration to the interpolated Eu value between Sm and Gd assuming no Eu anomaly.

** All Fe expressed as Fe203.

TABLE 1
(continued)

15	16A	17	19	20A	21	22A	23	24	25	26	27A	28A	29	30	31	32
49.73	49.87	49.88	50.27	50.28	50.83	50.84	50.85	50.86	50.95	51.11	51.55	51.74	52.42	52.73	52.88	52.98
1.73	0.76	0.74	0.80	1.54	2.83	1.83	1.73	1.41	1.10	1.48	1.07	1.11	0.94	0.98	1.00	1.64
14.51	17.35	17.43	16.94	15.01	14.91	15.16	15.75	14.81	16.23	16.21	16.75	16.22	15.56	15.96	16.13	16.05
1.85	0.88	1.29	1.41	2.24	2.03	1.13	1.47	2.82	1.64	1.27	1.59	2.22	2.30	2.93	2.31	0.99
13.86	9.33	7.81	8.72	12.24	11.86	9.63	9.17	11.46	8.89	9.21	9.38	8.51	11.12	9.59	10.35	8.68
0.15	0.17	0.13	0.15	0.32	0.24	0.20	0.20	0.24	0.18	0.18	0.14	0.14	0.21	0.21	0.20	0.17
6.86	8.95	7.54	7.23	5.83	5.35	7.47	6.42	5.05	7.12	6.70	7.79	6.64	5.52	4.49	5.19	6.28
7.79	10.00	11.51	11.41	7.30	9.01	11.41	10.84	10.18	10.24	10.30	7.59	11.10	9.24	9.64	8.54	9.91
2.56	2.12	2.84	2.37	4.27	2.06	1.53	2.67	2.64	2.88	2.92	3.52	1.33	2.38	2.89	2.81	2.38
0.29	0.21	0.28	0.39	0.27	0.50	0.39	0.45	0.54	0.50	0.46	0.15	0.21	0.37	0.33	0.17	0.36
0.17	0.08	0.09	0.10	0.16	0.29	0.14	0.17	0.18	0.12	0.20	0.14	0.15	0.10	0.13	0.14	0.19
99.50	99.72	99.54	99.79	99.46	99.91	99.73	99.72	100.19	99.85	100.04	99.67	99.37	100.16	99.88	99.72	99.63
0.44	0.61	0.60	0.56	0.42	0.41	0.56	0.52	0.39	0.55	0.54	0.56	0.53	0.43	0.40	0.43	0.54
0.63	0.72	0.69	0.73	0.49	0.71	0.80	0.69	0.68	0.66	0.66	0.54	0.82	0.68	0.65	0.63	0.70
664	295	268	298	427	338	321	294	429	313	333	314	332	356	321	275	237
7	304	242	204	21	47	247	230	25	222	185	229	144	24	20	24	192
18	59	49	44	17	36	91	54	17	59	53	63	51	12	10	11	51
134	72	62	84	165	135	99	101	134	81	89	61	89	122	111	131	91
20	17	16	16	20	23	19	18	19	16	18	18	17	18	19	20	19
4	9	3	4	5	6	4	8	4	5	2	2	3	3	3	2	4
157	224	221	175	105	165	179	276	184	214	136	141	179	160	141	193	263
27	14	11	13	28	53	32	31	21	18	27	19	20	14	16	16	34
54	29	26	27	67	227	74	125	42	51	83	60	64	21	21	23	165
1.8	1.0	1.7	1.7	2.0	5.6	1.6	3.0	1.5	1.5	2.7	2.4	2.3	0.9	1.1	0.8	5.1
85	370	177	89	44	104	52	83	37	149	62	15	37	90	19	11	50

7		3.2	3.4	9.0	12.9	3.2	9.2	4.4	5.2	7.7	6.2	8.2	4.1	2.4	1	13.8
16	12	8.6	8.9	26.3	35.0	9.8	22.7	10.5	14.2	18.4	16.9	18.8	9.1	9.1	15	30.6
		1.18	1.30	3.44	5.13	1.75	3.19	1.53	1.94	2.61	2.38	2.56	1.24	1.28		4.26
		5.4	6.2	15.7	26.0	10.3	15.6	8.0	9.4	13.1	11.4	11.8	6.1	6.4		19.5
		1.55	1.87	4.24	7.74	3.69	4.53	2.69	2.73	3.79	3.06	3.26	1.90	2.04		5.46
		0.69	0.71	2.10	2.55	1.52	1.79	1.12	0.99	1.29	1.35	1.08	0.93	1.05		1.75
		1.84	2.20	4.68	8.69	4.38	5.36	3.32	3.13	4.18	3.32	3.50	2.32	2.51		5.78
		0.32	0.37	0.81	1.58	0.85	0.92	0.58	0.55	0.76	0.55	0.58	0.41	0.42		1.00
		2.25	2.37	5.22	9.97	5.63	5.77	3.79	3.47	4.98	3.57	3.74	2.68	2.86		6.27
		0.46	0.53	1.09	2.11	1.20	1.24	0.81	0.74	1.06	0.76	0.81	0.61	0.62		1.32
		1.33	1.47	3.23	5.99	3.29	3.43	2.37	2.18	2.96	2.20	2.31	1.71	1.78		3.69
		0.18	0.20	0.47	0.88	0.49	0.50	0.35	0.30	0.44	0.33	0.34	0.25	0.25		0.55
		1.25	1.37	3.06	5.60	3.10	3.11	2.22	2.01	2.84	2.11	2.25	1.66	1.70		3.50
		0.19	0.22	0.47	0.87	0.48	0.48	0.34	0.30	0.43	0.31	0.34	0.26	0.27		0.52
		0.93	0.87	2.20	7.00		3.67	1.39	1.55		1.78	2.07	0.75	0.85		4.68
8	3	8	7	6	31	5	10	6	5	7	4	5	5	5	4	11
0	1	0.54	0.65	0.51	2.47	0.44	1.07	0.68	1.04	1.36	1.65	1.94	0.79	0.76	1	3.75
		0.18	0.17	0.41	0.74	0.09	0.34	0.34	0.24	0.33	0.34	0.34	0.26	0.23		1.00
		1.8	1.7	2.2	1.6	0.8	1.9	1.2	1.8	1.7	2.1	2.2	1.4	1.4		2.3
		1.26	1.07	1.44	0.95	1.15	1.11	1.15	1.03	0.99	1.30	0.98	1.35	1.42		0.95

Analytical methods are given in app. 1.
* Ratio of the chondrite-normalized Eu concentration to the interpolated Eu value between Sm and Gd assuming no Eu anomaly.
** All Fe expressed as Fe203.

TABLE 1
(continued)

		Intermediate Gneisses				Felsic Gneisses									
33	34	36	38	39	42	43	44	45	46	47	48	49	50	51	52
53.35	54.56	57.05	61.46	62.48	67.53	71.59	72.00	72.07	73.53	75.54	76.14	76.21	76.86	77.48	77.49
1.21	0.89	1.07	0.60	1.08	0.34	0.22	0.29	0.40	0.28	0.12	0.17	0.25	0.10	0.10	0.13
14.24	14.77	17.08	16.40	15.25	17.48	13.58	14.15	14.44	13.29	12.66	12.73	12.58	11.95	12.03	12.13
1.31	1.95	2.43	0.88	1.35	0.53	0.80	0.43	0.36	0.62	0.42	0.14	0.58	0.13	0.09	0.84
11.64	10.61	7.28	7.41	7.34	2.33	3.44	2.93	3.07	4.10	1.87	2.69	2.07	1.13	1.92	1.24
0.18	0.20	0.10	0.17	0.21	0.03	0.05	0.03	0.07	0.19	0.02	0.09	0.01	0.02	0.06	0.01
7.12	4.96	4.14	2.55	2.07	1.79	1.89	1.82	2.52	0.57	1.10	0.90	0.79	0.77	0.42	0.10
7.67	8.67	6.23	7.41	5.78	4.36	2.65	3.28	2.43	3.19	2.29	2.75	3.62	0.62	0.86	0.37
2.59	2.39	4.14	2.97	3.30	3.92	2.86	3.28	2.98	3.09	4.03	3.52	2.81	3.24	4.42	5.47
0.16	0.44	0.14	0.39	0.34	1.60	2.30	1.38	1.61	1.00	1.23	0.91	0.94	4.48	2.46	2.06
0.15	0.12	0.25	0.10	0.44	0.08	0.04	0.05	0.07	0.06	0.01	0.04	0.05	0.01	0.01	0.02
99.62	99.56	99.91	100.34	99.64	99.99	99.42	99.64	100.02	99.92	99.29	100.08	99.91	99.31	99.85	99.86
0.50	0.42	0.44	0.36	0.30	0.53	0.45	0.49	0.57	0.18	0.47	0.36	0.35	0.52	0.27	0.08
0.62	0.67	0.45	0.58	0.49	0.38	0.34	0.36	0.31	0.36	0.24	0.30	0.42	0.10	0.10	0.04
400	344	273	175	6	68	6	26	41	0	0	0	7	2	0	0
10	14	50	3	2	9	8	0	23	2	2	2	1	1	1	0
18	11	22	5	6	7	4	8	10	4	6	6	8	3	6	4
113	101	59	94	160	37	101	71	79	100	52	129	53	57	63	52
19	18	20	18	21	18	17	16	17	17	14	19	12	14	15	13
3	5	2	4	5	50	73	31	44	19	33	29	34	87	55	22
197	156	223	155	158	289	87	146	153	80	189	188	145	55	74	46
23	12	88	17	38	3	44	31	35	35	44	58	24	49	54	40
54	18	69	63	77	48	231	164	137	112	186	201	125	158	194	181
2.0	1.3	1.1	2.7	1.2	3.6	3.6	3.8	3.4	2.4	3.9	4.3	4.4	5.3	4.3	4.7
86	59	17	110	53	478	322	221	244	218	550	243	386	573	595	519

6.5	5	10	8	9	2	16.7	15.6	21.3	15.6	22.1	26.5	12.9	27.8	30.6	24.7
16.9	11	28	28	22	21	39.8	33.0	43.5	29.7	60.8	59.9	29.4	63.4	66.6	56.5
2.30						5.16	4.14	5.28	3.87	6.24	7.83	3.25	7.08	7.59	6.90
11.3						23.3	18.6	22.6	17.6	26.4	34.6	13.2	29.2	32.3	29.3
3.27						6.73	5.08	5.72	5.23	6.81	9.22	3.44	6.68	7.48	7.41
1.16						1.49	1.12	1.23	1.54	1.01	1.80	0.84	0.68	1.62	1.13
3.68						7.95	5.64	5.98	5.95	7.13	10.29	3.57	7.23	7.66	7.70
0.63						1.51	0.99	0.98	1.10	1.33	1.78	0.68	1.29	1.41	1.33
4.18						10.34	6.54	6.36	7.32	9.32	11.46	4.44	9.09	9.94	8.54
0.90						2.35	1.44	1.42	1.65	2.17	2.53	1.04	2.13	2.34	1.91
2.52						7.06	4.22	4.41	4.85	6.60	7.42	3.14	6.57	7.00	5.60
0.37						1.14	0.67	0.69	0.76	1.11	1.18	0.48	1.04	1.14	0.89
2.38						7.29	4.45	4.73	4.89	7.12	7.43	3.20	6.68	7.48	5.71
0.37						1.13	0.70	0.74	0.75	1.12	1.15	0.52	1.03	1.17	0.90
1.83						7.32	5.41	5.17	3.54	6.18	6.43	3.78	5.68	6.25	5.77
6	5	6	11	4	8	7	9	11	6	6	12	8	12	5	7
1.20	1	2	2	2	2	5.00	4.69	5.31	3.01	8.32	7.26	5.32	6.37	8.94	7.70
0.35						1.20	1.48	1.36	0.69	2.07	1.84	1.68	1.59	1.58	1.63
1.8						1.4	1.9	2.4	1.6	2.2	2.1	2.4	2.5	2.3	2.6
1.02						0.62	0.64	0.65	0.84	0.44	0.56	0.74	0.30	0.65	0.46

Analytical methods are given in app. 1.

* Ratio of the chondrite-normalized Eu concentration to the interpolated Eu value between Sm and Gd assuming no Eu anomaly.

** All Fe expressed as Fe203.

TABLE 2

Norms and modes for the Partridge Formation volcanics

	Amphibolites															
SAMPLE	O	1	2A	3A	90	4	5A	6	7	8A	9	10	11	12A	13A	14A
Qz															1.90	
Ol	31.41	22.51	13.11	17.23	11.99	16.02	18.86	13.05	13.30	15.09	14.87	9.33	14.95	25.83		4.23
Cor																
CPX	13.80	17.11	23.50	14.46	11.60	10.40	19.51	14.28	20.63	11.76	17.41	15.06	20.69	2.77	23.28	16.05
OPX	4.87	1.85	6.82	9.49	14.77	16.24	3.27	9.68	9.88	15.17	5.01	18.05	4.35		19.72	17.57
Ne														1.97		
Or	1.14	1.83	1.95	1.24	0.83	0.77	4.20	3.26	1.30	6.50	1.71	1.77	1.71	17.91	1.66	0.95
Plag	45.59	52.49	49.71	54.35	58.01	51.17	50.36	54.22	50.92	46.09	57.66	51.28	54.51	45.51	49.82	53.76
Mt	1.79	1.74	1.94	1.48	1.41	1.84	1.47	2.19	1.50	1.88	1.41	1.64	1.39	2.24	1.62	1.95
Ilm	1.08	1.67	1.90	1.18	1.25	2.59	1.67	2.55	1.52	2.70	1.06	1.63	1.37	2.94	1.81	4.50
Ap	0.17	0.24	0.26	0.17	0.17	0.33	0.17	0.29	0.17	0.43	0.19	0.24	0.19	0.40	0.31	0.64
Mg'	75	68	59	72	71	70	72	51	71	67	68	68	70	54	61	58
An'	71	68	71	76	75	59	64	55	67	62	60	63	58	41	81	52
DI	14	18	16	14	15	21	22	27	18	24	24	20	24	46	13	26
Estimated mineral modes.																
Quartz			t			t		3		t				5	5	
Plagioclase	7	14	27	23	33	32	23	48	25	32	35	28	29	30	38	35
K-feldspar								tr								
Biotite		t		t			2	t		5	t	t	t	25	t	t
Muscovite																
Hornblende	78	85	55	75	60	60	75	45	75	60	65	70	70	25	50	60
Cummingtonite				1	5	t				2		t		15		
Orthoamphibole	15	1				6										

Clinopyroxene			13													3	
Orthopyroxene																	
Garnet																	
Fe3+-zoisite			t													1	
Clinozoisite			t														
Pistacite																	
Ilmenite	t	t	1	t	1	1	t	1	t	1		1		t			3
Magnetite								3									
Sulfide				t		1	t	t	t			t			2		t
Rutile				t	t	t			t				t		tr		
Sphene			1						t				1		1		1
Zircon						t	t	t		t	t	t	t?	t			t
Allanite						t								t			t
Apatite		t	t	t	t	t	t	t	t	t	t	t	t	t	t		1
Chlorite				1r	1r		tr				tr	tr	tr				
Talc	tr	tr?	2r	tr?													
Sericite	tr	tr	tr			tr	tr	tr	tr	tr	tr	1r	tr	tr	tr	tr	tr
Calcite			1						t								

All norms calculated assuming molar Fe3+/Fetotal = 0.1.
Mg′ = molar Mg/(Mg/Fe) in normative silicates.
An′ = anorthite % in normative plagioclase.
DI = Differentiation index: (Qz+Or+Ab+Ne)/Total.
Sample 45 also contains 3% sillimanite and trace staurolite.
t = trace amount present, usually ≪ 1%.
r = mineral appears to be of retrograde origin.

TABLE 2

(continued)

15	16A	17	19	20A	21	22A	23	24	25	26	27A	28A	29	30	31	32	33
					5.44	3.72		0.34				6.74	3.70	3.30	4.27	5.41	4.92
1.00	5.42	11.97	5.30	16.32			0.22		6.26	3.31	6.59						
8.58	9.70	18.42	17.68	11.87	10.72	18.31	18.95	18.82	16.56	16.48	5.98	13.55	12.15	14.63	8.84	13.04	8.54
33.11	24.97	6.40	16.64	6.92	25.12	23.59	20.25	23.12	15.75	18.11	22.85	24.71	27.11	21.72	26.65	21.78	31.84
1.71	1.24	1.66	2.31	1.60	2.96	2.30	2.66	3.20	2.96	2.72	0.89	1.24	2.19	1.95	1.01	2.13	0.95
48.91	55.13	58.03	54.50	57.16	47.41	46.29	52.27	49.37	54.28	54.48	59.27	48.97	50.86	54.14	54.72	52.18	48.67
2.50	1.63	1.45	1.61	2.30	2.21	1.72	1.69	2.26	1.67	1.67	1.74	1.69	2.13	1.97	2.00	1.54	2.07
3.29	1.44	1.41	1.52	2.93	5.38	3.48	3.29	2.68	2.09	2.81	2.03	2.11	1.79	1.86	1.90	3.11	2.30
0.40	0.19	0.21	0.24	0.38	0.69	0.33	0.40	0.43	0.28	0.47	0.33	0.36	0.24	0.31	0.33	0.45	0.36
51	66	66	62	49	51	64	60	45	61	61	62	59	48	45	48	62	56
54	66	57	62	35	62	71	55	53	54	53	48	76	59	53	55	60	54
24	19	26	22	38	26	19	25	26	27	27	31	19	26	30	29	28	28
3			5	7	6	8	4	2	3	1		10	5	7	10	5	4
24	62	40	45	42	37	30	39	32	40	47	43	34	29	36	35	40	49
					tr												
1	3		t	t	t		t	t	2	1	t			t	tr	3	t

50 20	25 10	60	50	45 3	50	60	55	65	55	50	35 20	55	60	55	49 t	50	25 20
					4								5		5		1
2 t *	t	t	t	1 2	3 t tr	1	1	1 t	t	1 t	2	1	1	1 1	1	2 t	1 t
t		t t	t	t	t	1	1 t	t t	t	t	t	t	t	t	t	t	t
t	t	t	t	t	t t	t	t	t	t t	t	t t	t t	t	t	t	t t	t t
					tr		tr										
	tr	tr	tr	tr	tr	tr	tr	tr	tr	tr	tr	tr	tr	tr	tr tr	tr	tr

All norms calculated assuming molar Fe3+/Fetotal = 0.1.
Mg′ = molar Mg/(Mg/Fe) in normative silicates.
An′ = anorthite % in normative plagioclase.
DI = Differentiation index: (Qz+Or+Ab+Ne)/Total.
Sample 45 also contains 3% sillimanite and trace staurolite.
t = trace amount present, usually ≪ 1%.
r = mineral appears to be of retrograde origin.

TABLE 2
(continued)

	Intermediate Gneisses				Felsic Gneisses									
34	36	38	39	42	43	44	45	46	47	48	49	50	51	52
8.07	7.98	19.03	22.32	25.06	34.95	35.88	37.64	40.96	39.36	43.10	45.82	37.59	38.51	35.60
				1.56	1.66	1.42	3.54	1.47	0.56	1.05	0.48	0.67	0.56	0.28
11.70	1.39	4.94	0.01											
24.70	22.84	15.98	17.12	8.34	10.93	9.29	11.04	8.58	6.09	6.52	5.62	3.74	4.12	3.17
2.60	0.83	2.30	2.01	9.46	13.60	8.16	9.51	5.91	7.27	5.38	5.56	26.47	14.54	12.18
48.52	62.73	55.39	53.74	54.29	37.10	43.70	36.81	41.58	45.40	43.16	41.42	30.43	41.60	48.02
1.99	1.53	1.32	1.38	0.45	0.67	0.53	0.55	0.75	0.36	0.45	0.42	0.20	0.32	0.32
1.69	2.03	1.14	2.05	0.65	0.42	0.55	0.76	0.53	0.23	0.32	0.47	0.19	0.19	0.25
0.28	0.59	0.24	1.04	0.19	0.09	0.12	0.17	0.14	0.02	0.09	0.12	0.02	0.02	0.05
47	51	41	36	60	50	56	63	21	52	41	42	58	31	10
57	43	53	47	38	33	35	30	36	24	30	41	9	10	3
31	44	46	52	68	73	72	72	73	81	78	75	92	91	94
7	33	15	20	25	30	30	40	40	40	40	40	45	40	35
39	47	49	55	61	58	60	48	46	55	52	48	13	34	40
							t?					35	20	20
t	1	t	5	10	10	8	7	8	5	5	12	6	4	4

				3		tr	tr	2r				t		t
50	8	30	12											
	3													
	5													
3		5	5	t		2	2	3		3			2	
										tr				
					t		tr				tr			
1		1	2	t	1r			t				t		
	2										t			1
t	t	t	t	t				t		t		t	t	
				tr			tr							
t	t	t	t	t	t	t	t	t	t	t	t	t	t	t
	t	t	t	t?		t		t	t	t	t	t	t	
t	1	t	1	t	t	t	t	t	t	t	t	t	t	t
				1r	1r	tr	tr	tr	tr	tr				tr
	tr	tr	tr	tr	tr	tr	tr	1r	tr		tr	1r	tr	tr
							tr							

All norms calculated assuming molar Fe3+/Fetotal = 0.1.
Mg' = molar Mg/(Mg/Fe) in normative silicates.
An' = anorthite % in normative plagioclase.
DI = Differentiation index: (Qz+Or+Ab+Ne)/Total.
Sample 45 also contains 3% sillimanite and trace staurolite.
t = trace amount present, usually ≪ 1%.
r = mineral appears to be of retrograde origin.

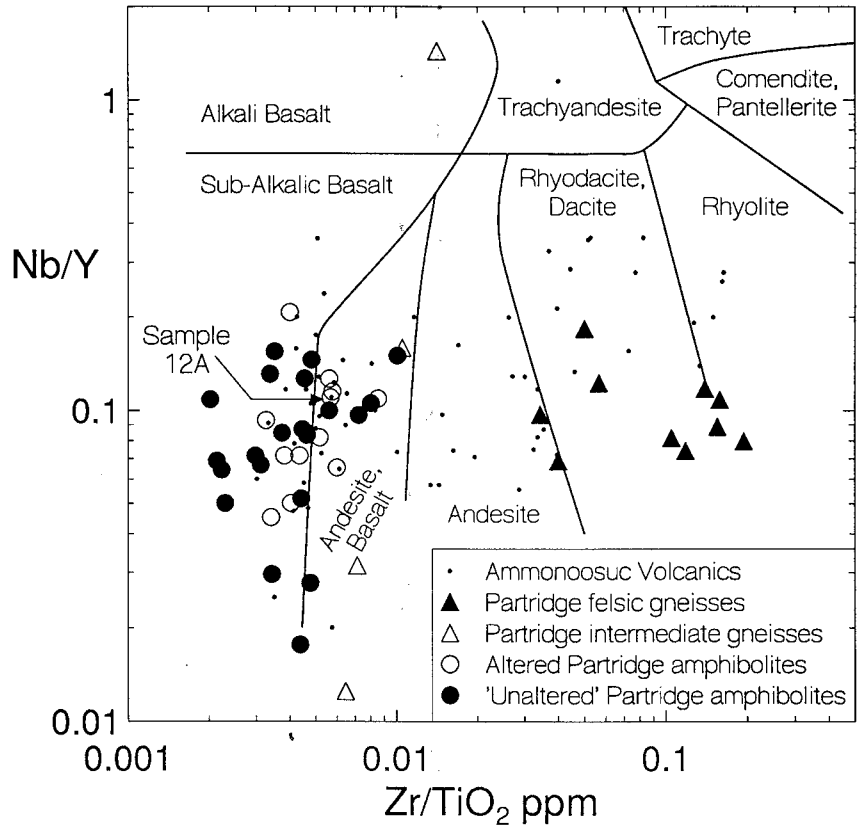

Fig. 3. Igneous rock classification diagram using immobile trace elements (Winchester and Floyd, 1977) with data plotted from the Ammonoosuc Volcanics and Partridge Formation.

potential pre- and synmetamorphic chemical alteration, classification schemes using the major elements and schemes using immobile elements consistently show that the Ammonoosuc and Partridge volcanics are a subalkaline suite with protoliths ranging from tholeiitic basalt for the amphibolites, to dacite, rhyodacite, and rhyolite for the felsic gneisses (Schumacher, 1988; Hollocher, ms).

Despite the consistency of classifying the protoliths of the Partridge volcanics, these are not pristine igneous rocks, and it is important to estimate the extent of pre- or synmetamorphic chemical alteration that may have affected them. This has been discussed at length for the Ammonoosuc Volcanics (Schumacher, ms and 1988) and for volcanics in the Partridge Formation (Hollocher, 1985 and ms). Hollocher (ms) found that the Partridge amphibolites formed a single geochemically

coherent group based on the relatively immobile elements (such as Ti, Zr, Y, and Nb, hereafter referred to as immobile elements). Some amphibolites, however, had anomalous concentrations of some mobile elements (Mg, Ca, Na, K). These anomalous amphibolites were related to the rest of the amphibolites by igneous processes such as olivine accumulation or by chemical alteration processes including high-temperature hydrothermal seawater alteration, low-temperature sea water alteration (submarine weathering), subaerial weathering, and contamination with calcareous material. Twelve of the 35 Partridge amphibolites are here classified as having been altered by post-eruptive processes using the methods of Hollocher (1985b). These samples have an "A" suffix in their sample numbers.

In none of the amphibolites is there evidence that the concentrations of elements other than the most mobile (Mg, Ca, Na, K, Sr, Ba, Rb) have changed significantly from their igneous protoliths. If this had not been the case, differential change in the concentrations of presumed immobile elements would have destroyed the geochemical coherence of the amphibolite group. I do not suggest that the "unaltered" amphibolites have experienced no chemical change since eruption, but since the mobile and immobile elements tell the same story, these samples are considered here to be "unaltered" for practical purposes. Note that in most cases the compositions of altered and "unaltered" Partridge amphibolites are similar, as shown in the figures below, indicating that even the altered samples are not too dissimilar from their original compositions for most elements.

Schumacher (1988) was able to differentiate between severely altered and other felsic rocks in the Ammonoosuc Volcanics on the basis of variations in Ca, Na, and K relative to Al (fig. 4). In figure 4, subalkaline felsic igneous rocks plot close to the "Plagioclase line," which defines the chemical variation in quartz + plagioclase ± K-feldspar rocks. Most chemical alteration processes in quartzofeldspathic igneous rocks produce clay, chlorite, or fine-grained white mica, which are enriched in Al compared to the original feldspars, biotite, and amphibole. Such alteration will move the composition of a felsic igneous rock toward the origin in figure 4. On this basis, Schumacher identified 7 of 29 felsic Ammonoosuc samples as having altered compositions.

Nine of the ten analyzed felsic Partridge gneisses lie close to the "Plagioclase line" in figure 4, and only sample 45 is notably displaced toward the origin. Sample 45 is the most Al-rich Partridge felsic gneiss (14.44 percent Al_2O_3) and was previously interpreted as coming from a metamorphosed weathering horizon on a thick felsic volcanic layer (Peter Robinson, oral communication, 1982). Even sample 45 lies within the field of felsic igneous rocks (fig. 4) and so cannot be clearly identified as having been altered on this basis. Since all ten Partridge felsic gneisses occur within the field of igneous rocks in figure 4 and form a relatively coherent chemical group for both mobile and immobile elements, these samples are here considered to be "unaltered" for practical purposes.

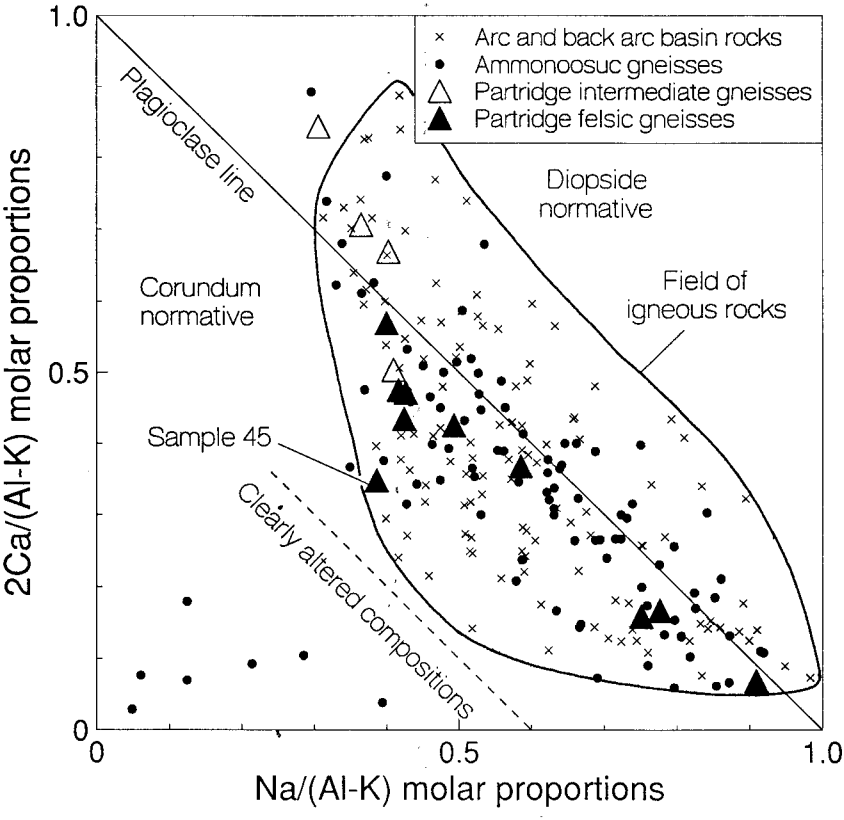

Fig. 4. Diagram used to distinguish between highly altered and less altered or unaltered intermediate and felsic gneisses in the Ammonoosuc Volcanics and Partridge Formation (after Schumacher, 1988). The vertical and horizontal axes are measures of the normative anorthite and albite components, respectively. Rocks with only normative quartz and feldspars plot along the "Plagioclase line," with diopside-normative rocks to the upper right and corundum-normative rocks to the lower left. The dashed line shows the approximate limit of fresh subalkalic felsic rock compositions associated with island arcs having SiO_2 >63 percent (Purman and Alfors, 1969; Lowder and Carmichael, 1970; Arculus, 1976; Hildreth, 1981; Mahood, 1981; Smith and Johnson, 1981; Dixon and Stern, 1983; Meijer, 1983; Merzbacher and Eggler, 1984; Noble and others, 1984; Robinson, Brem, and McKee, 1984; Bice, 1985; Reagan and Meijer, 1984; Swanson and McDowell, 1985; Vennum and Rowley, 1986; Box and Patton, 1989; Ikeda and Yuasa, 1989).

AMPHIBOLITE GEOCHEMISTRY

The Partridge amphibolites follow chemical variation trends similar to those of modern basalts and basaltic andesites (figs. 5 and 6; Hollocher ms). Twenty three of the 35 amphibolites are olivine–OPX–normative, 11 are quartz–OPX–normative, and one is olivine–nepheline–normative (sample 12A). The seemingly alkalic sample 12A probably has normative nepheline as a result of low-temperature seawater alteration, which

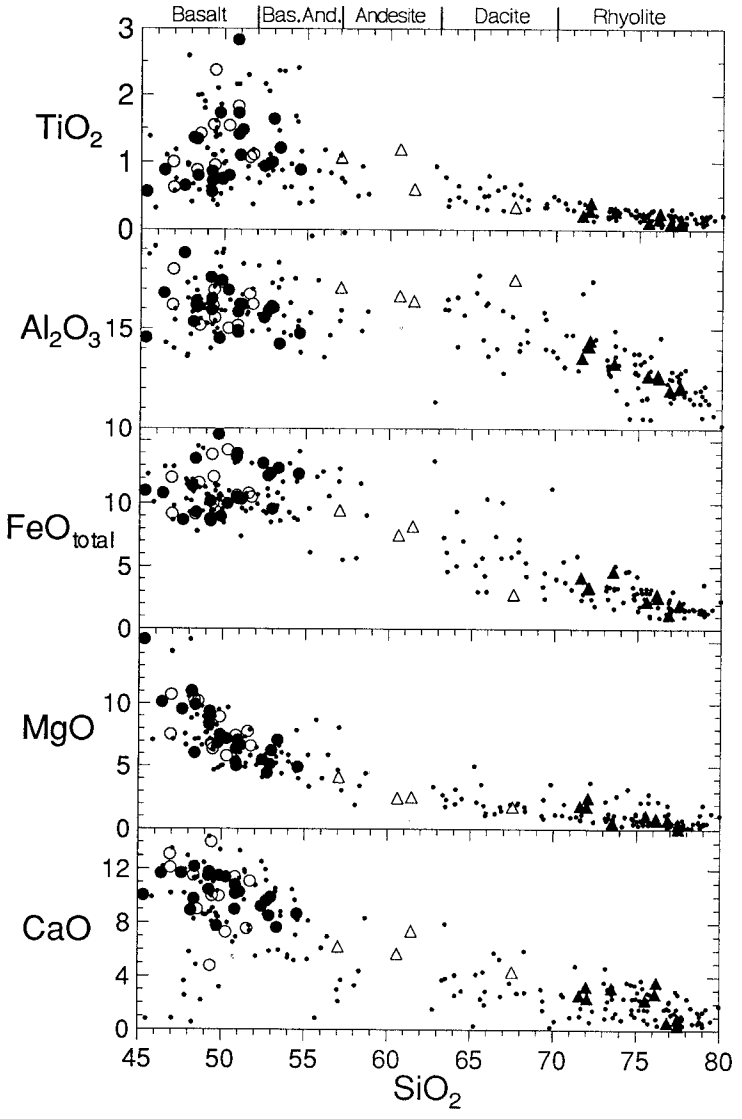

Fig. 5. Major element-SiO_2 chemical variation diagrams showing data from the Ammonoosuc Volcanics and volcanics in the Partridge Formation. A few samples of Ammonoosuc Volcanics having very high concentrations of SiO_2 or other elements are not shown. Nominal igneous rock classifications are modified after LeBas and others (1986). See figure 6 for explanation of symbols.

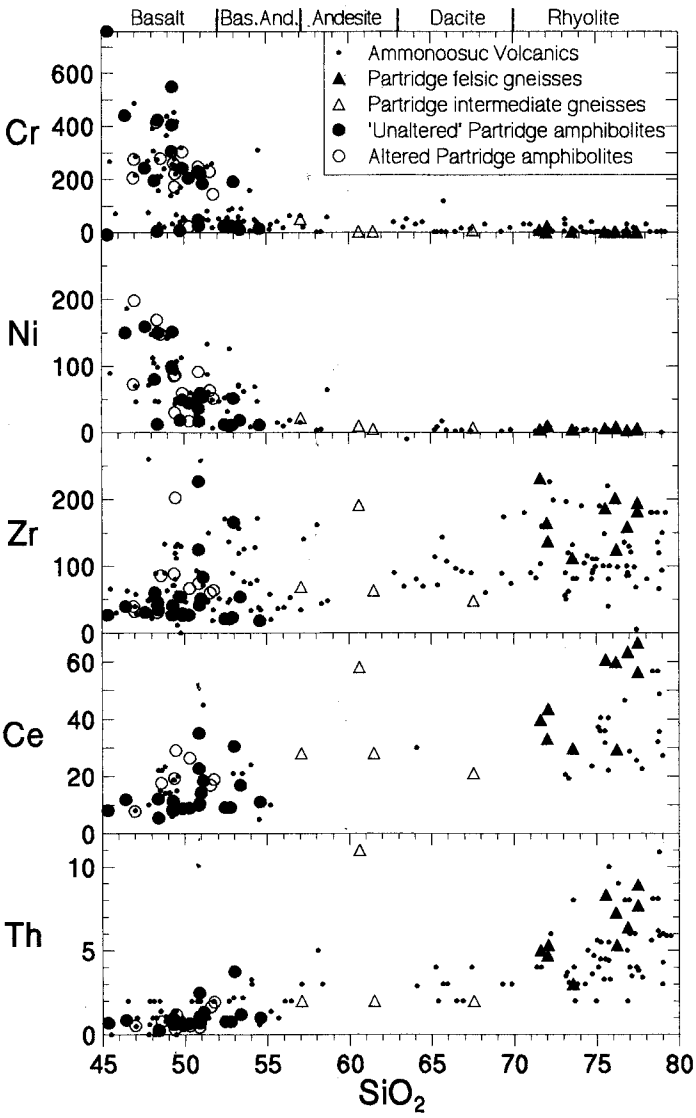

Fig. 6. Trace element-SiO_2 chemical variation diagrams, showing data from the Ammonoosuc Volcanics and volcanics in the Partridge Formation. A few samples of Ammonoosuc Volcanics having very high concentrations of SiO_2 or other elements are not shown. Nominal igneous rock classifications are modified after LeBas and others (1986).

enriched the rock in K and Na and depleted it in Ca relative to the other amphibolites (Hollocher, ms). Sample 12A is otherwise similar in composition to the other amphibolites and besides normative nepheline does not have alkalic characteristics (fig. 3, for example).

The Partridge amphibolites form a chemically continuous group without consistent composition gaps. Highly compatible elements such as Cr and Ni have extreme ranges of concentration that are probably the result of igneous fractionation and accumulation of olivine and chromite (Hollocher, ms). Less compatible elements such as Ca, Na, and Fe range in concentration by factors of about two, and Mg by a factor of three. Incompatible elements such as Zr, Ce, and Ti range in concentration by factors of about six. Ratios of immobile incompatible elements vary by factors of about four, although some of this variation is caused by analytical uncertainty at low concentrations. In contrast to the relatively small variation in most incompatible element ratios, there are large variations in the ratios of incompatible elements to Th (factor of 11) and U (factor of 18). The large variation of these ratios is only partly due to analytical uncertainty, and its origin is not understood.

The assignment of amphibolites in the Ammonoosuc Volcanics (considered here to be similar to Partridge amphibolites) to the tholeiitic or calc-alkaline series has not been consistent among various studies. Schumacher (ms), Aleinikoff (1977), Shumway (ms), and Leo, Zartman, and Brookins (1984) assigned the Ammonoosuc amphibolites to the tholeiitic series. Leo (1985) described his set of Ammonoosuc amphibolites as being calc-alkaline, and Leo (1991) described a new set of samples as being "marginally tholeiitic" but lacking an Fe-enrichment trend. According to figure 7 the Partridge amphibolites appear to be tholeiitic, which is consistent with their subalkalic character (fig. 3) and low absolute K_2O contents (all but two ≤ 0.71 percent). In particular, the Partridge amphibolites have a short but clear Fe-enrichment trend (fig. 7A and C) and a strong Cr-depletion trend (fig. 7B), both characteristic of tholeiitic suites. Ammonoosuc amphibolites cluster around the Partridge amphibolites but have significant scatter, probably due in part to chemical alteration. Alteration effects would be particularly evident in figure 7A, in which a small gain of alkalis (from sea water) would cause tholeiitic rocks to cross into the calc-alkaline field. This is apparently the case for Partridge sample 12A (Hollocher, ms). Since the great majority of Ammonoosuc amphibolites lie in tholeiitic fields it is reasonable to assign these rocks to the tholeiitic series along with the Partridge amphibolites.

Figure 8, A and B, show REE patterns for the 26 Partridge amphibolites for which REE data are available. Samples 7 and 22A are depleted in light rare earth elements (LREE), have Ce_n/Yb_n ratios of ~ 0.8, and Gd_n abundances 9.1x and 16.9x chondrites, respectively. Both LREE-depleted samples have small positive Eu anomalies. The other 24 plotted samples have nearly straight, slightly LREE-enriched patterns with Ce_n/Yb_n ratios of 1.1 to 2.3 and Gd_n abundances of 6x to 34x chondrites. Of

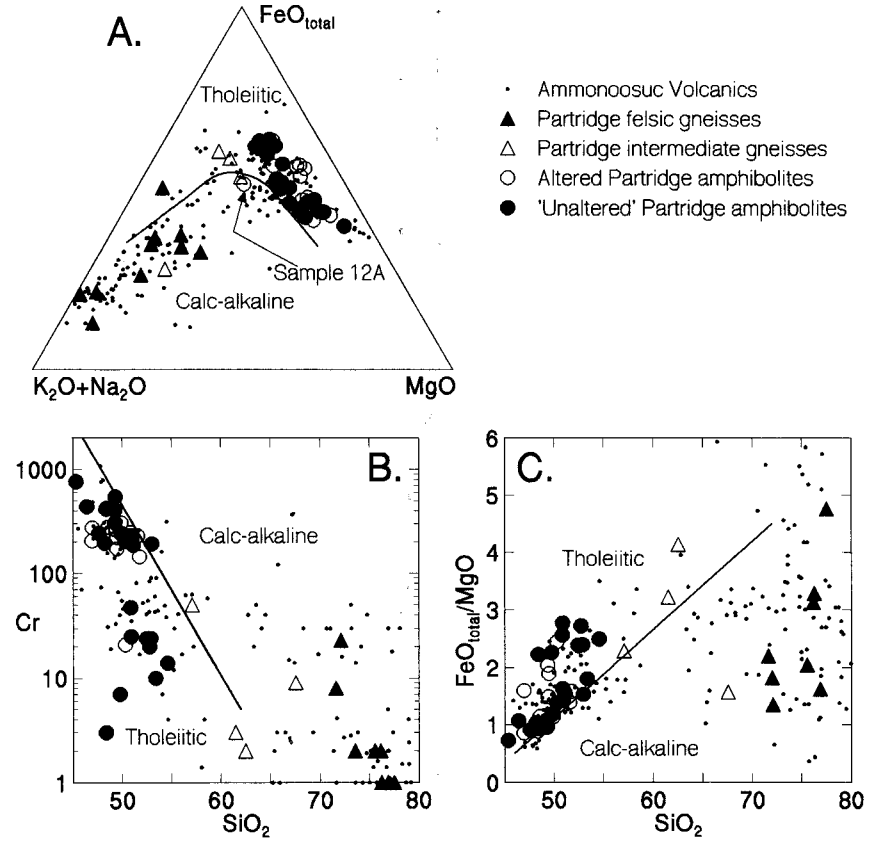

Fig. 7. Diagrams that discriminate between the tholeiitic and calc-alkaline igneous series applied to the Partridge Volcanics, with the Ammonoosuc Volcanics shown for comparison. (A) is from Irvine and Baragar (1971), and (B) and (C) are from Miyashiro and Shido, 1975.

the 24 LREE-enriched samples, 13 have slight positive Eu anomalies ($Eu_n/Eu^* = 1.05$-1.44), 4 have slight negative anomalies ($Eu_n/Eu^* = 0.94$-0.95), and 7 have no significant anomalies ($Eu_n/Eu^* = 0.96$-1.04). Note that there are no consistent differences between the REE patterns of the altered compared to the "unaltered" amphibolites. The LREE-enriched Partridge amphibolites have REE patterns similar to those of Ammonoosuc amphibolites (Leo, 1985, 1991). The slightly LREE-enriched and LREE-depleted patterns of the Partridge amphibolites, having minor but commonly positive Eu anomalies, are similar to the REE patterns of many tholeiitic basalts from island arcs, back-arc basins, and mid-ocean ridges (Hawkins, 1977; Johnson and Arculus, 1978; Weaver and others, 1979; Basaltic Volcanism Study Project, 1981, figs. 1.2.5.14, 1.2.5.15, 1.2.7.9,

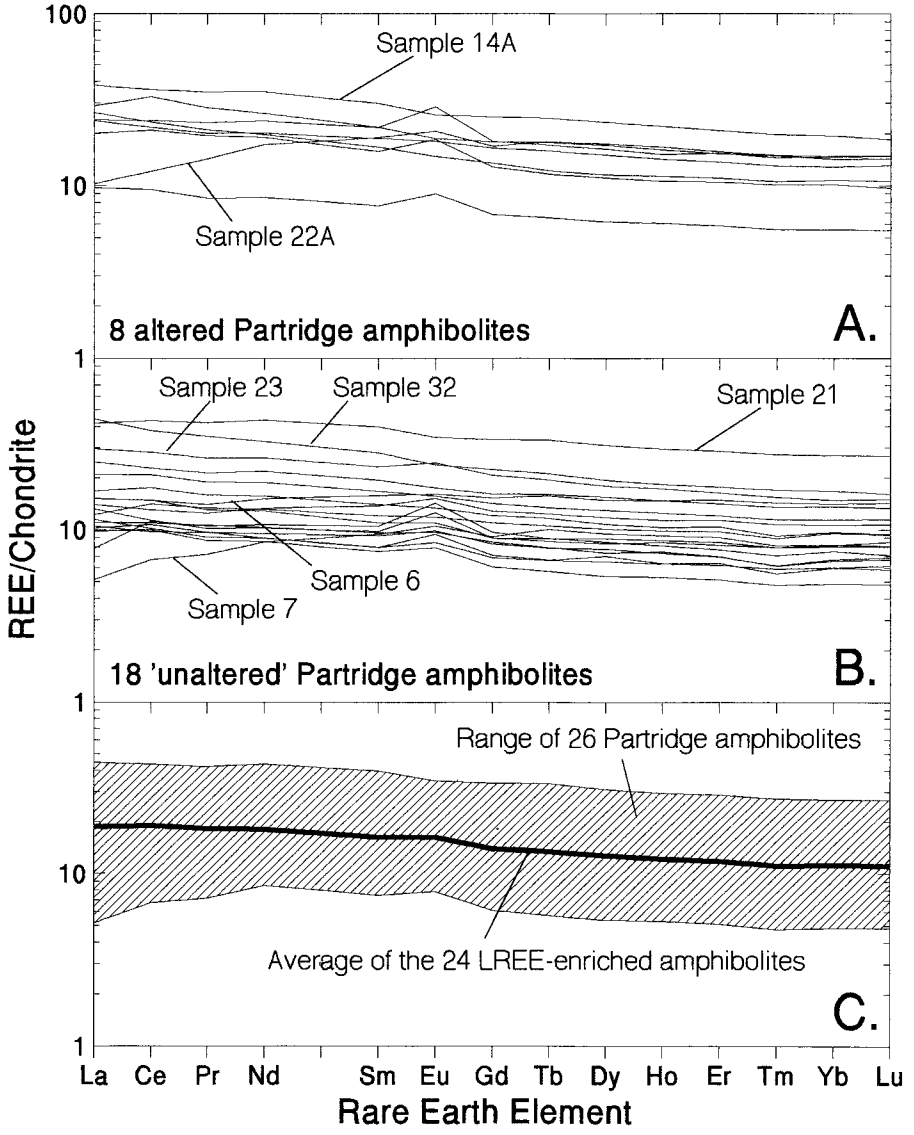

Fig. 8. Rare earth element diagrams for the Partridge amphibolites. (A) Altered Partridge amphibolites. (B) "Unaltered" Partridge amphibolites. Note the lack of systematic differences between the REE patterns of altered and "unaltered" amphibolites. (C) Comparison of the range of REE patterns for the all Partridge amphibolites with the average of all LREE-enriched amphibolites. Average line excludes LREE-depleted samples 7 and 22A. Normalizing values are given in table 3.

1.2.7.10; Marcelot and others, 1983; Hawkins and Melchior, 1985; Ikeda and Yuasa, 1989; Stern and others, 1990).

Figure 9, A and B, are spider diagrams for the Partridge amphibolites. Note that most of the scatter of the mobile elements (Rb, Ba, K, Sr) is in a few samples. In the remaining samples the scatter of the mobile elements is about the same as the scatter of the immobile elements. Looking principally at the elements U to Ce, Pr to Nd, and Sm to Lu (fig. 9C), the Partridge amphibolites have slightly incompatible element-enriched patterns on which are superimposed prominent negative Nb anomalies present in all samples. Most samples also have small negative anomalies for Hf and Zr. Samples 14A, 21, 23, and 32 have no Hf and Zr anomalies and are also the most enriched in the more compatible elements in this diagram and in figure 8. Other generalizations are difficult to make.

The details of the spider patterns in figure 9 vary considerably, but some comparisons can be made with modern rocks. The relatively flat to slightly incompatible element-enriched patterns with large negative Nb anomalies in figure 9 are common in basalts from island arcs (Sun, 1980; Briqueu, Bougault, and Joron, 1984; Thompson and others, 1984), and to a lesser extent in basalts from back-arc basins (Tarney, Saunders, and Weaver, 1977; Weaver and others, 1979; Marcelot and others, 1983; Hawkins and Melchior, 1985). Small negative Hf and Zr anomalies are also found in some island-arc basalts (Thompson and others, 1984; Briqueu, Bougault, and Joron, 1984).

FELSIC GNEISS GEOCHEMISTRY

The Partridge felsic gneisses are all slightly corundum-normative and are compositionally similar to dacite, rhyodacite, and rhyolite (table 1, figs. 3, 5, and 6). These gneisses have concentrations of highly compatible elements such as Cr and Ni that are much smaller than the Partridge amphibolites, concentrations of moderately compatible elements (in felsic systems) such as Ti, Fe, Mg, and Ca that are 4 to 10x smaller, and concentrations of incompatible elements such as Zr and Ce that are 2 to 5x larger. The Partridge felsic gneisses plot almost exclusively in the calc-alkaline fields of figure 7, as do the great majority of felsic Ammonoosuc rocks, so all probably belong to the calc-alkaline series.

REE patterns for the Partridge felsic gneisses are shown in figure 10A. These patterns are nearly flat in the middle rare earth (MREE) and heavy rare earth (HREE) regions and are LREE-enriched with Ce_n/Yb_n ratios of 1.4 to 2.6. Some samples are slightly depleted in MREE with respect to HREE. All felsic gneisses have pronounced negative Eu anomalies with Eu_n/Eu^* ratios of 0.29 to 0.83, in contrast to the positive Eu anomalies typical of the amphibolites. The range of normalized REE concentrations for the felsic gneisses is about a factor of two to three, smaller than the range of a factor of eight for the amphibolites. REE patterns for the Partridge felsic gneisses are essentially the same as lithologically similar rocks in the Ammonoosuc Volcanics (Leo, 1985,

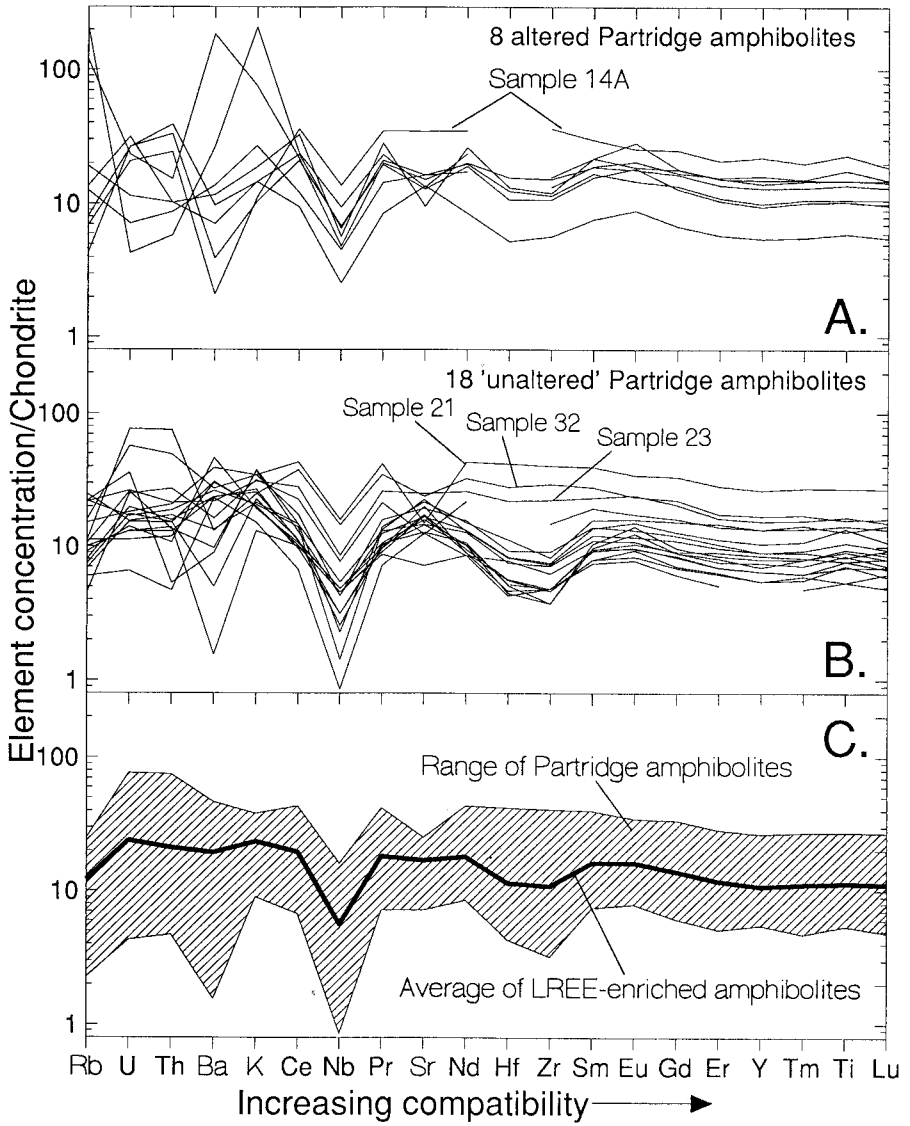

Fig. 9. "Spider" diagrams showing the chemical variation for altered Partridge amphibolites (A) and "unaltered" amphibolites (B). Except for wide variations in the concentrations of the mobile elements Rb, Ba, and K there are no systematic differences between the patterns of altered and "unaltered" amphibolites. Gaps represent missing values for Hf or Y. (C) The composition range for all amphibolites, exclusive of the mobile elements (Rb, Ba, K, Sr) in the altered amphibolites. The average includes all samples exclusive of the mobile elements in altered amphibolites and XRF values for La, Ce, and Th. The sequence of elements is from Hoffman (1988), although several elements in his sequence are omitted. Normalizing values are given in table 3.

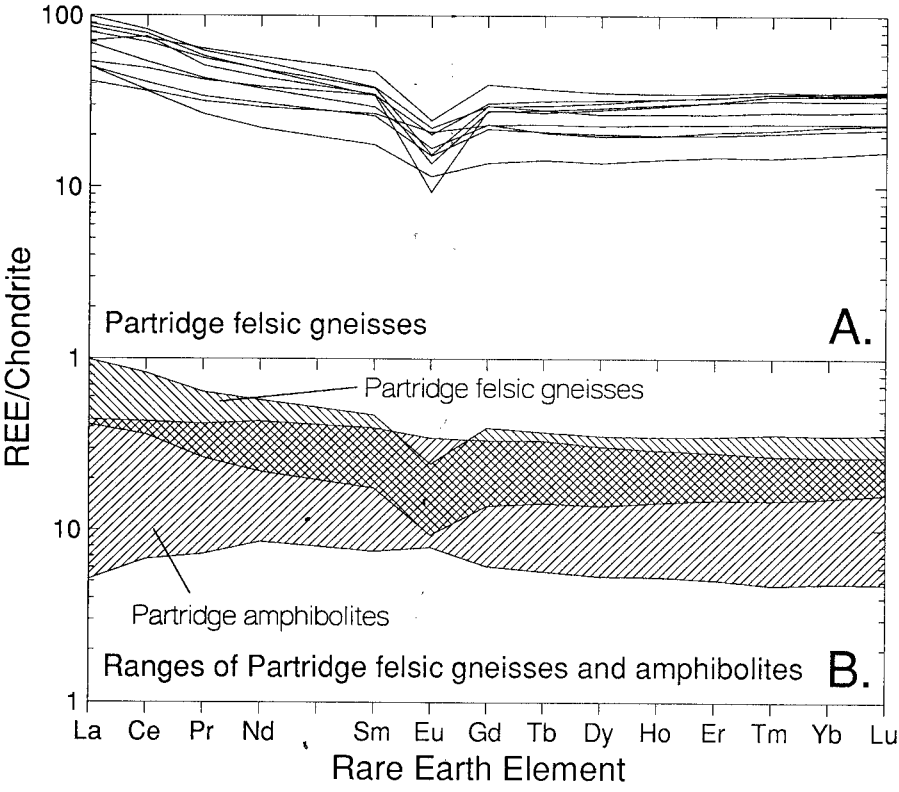

Fig. 10(A) Rare earth element diagram for the Partridge felsic gneisses. (B) Comparison of the range of Partridge felsic gneiss REE patterns with the REE pattern range of the Partridge amphibolites. Normalizing values are given in table 3.

1991). Modern felsic arc volcanics commonly have REE patterns similar to those of the Partridge felsic gneisses (Johnson and Arculus, 1978; Gill and Stork, 1979; Box and Patton, 1989). Except for the lack of a significant Eu anomaly in some cases, felsic volcanics from back-arc basins have REE patterns similar to those of the Partridge felsic gneisses (Weaver and others, 1979; Ikeda and Yuasa, 1989).

Figure 11A is a spider diagram for the Partridge felsic gneisses. The mobile elements (Rb, Ba, K, Sr) have concentration variations not much larger than many of the plotted immobile elements, consistent with the interpretation that these rocks have relatively unaltered compositions. The felsic gneisses are generally enriched in the less compatible elements by factors of about 100 with respect to chondrites and are enriched in the more compatible elements by factors of about 20. There are pronounced negative Nb, Sr, Eu, and Ti anomalies. Negative Sr, Eu, and Ti anomalies are common for felsic magmas in most geologic environments. Negative

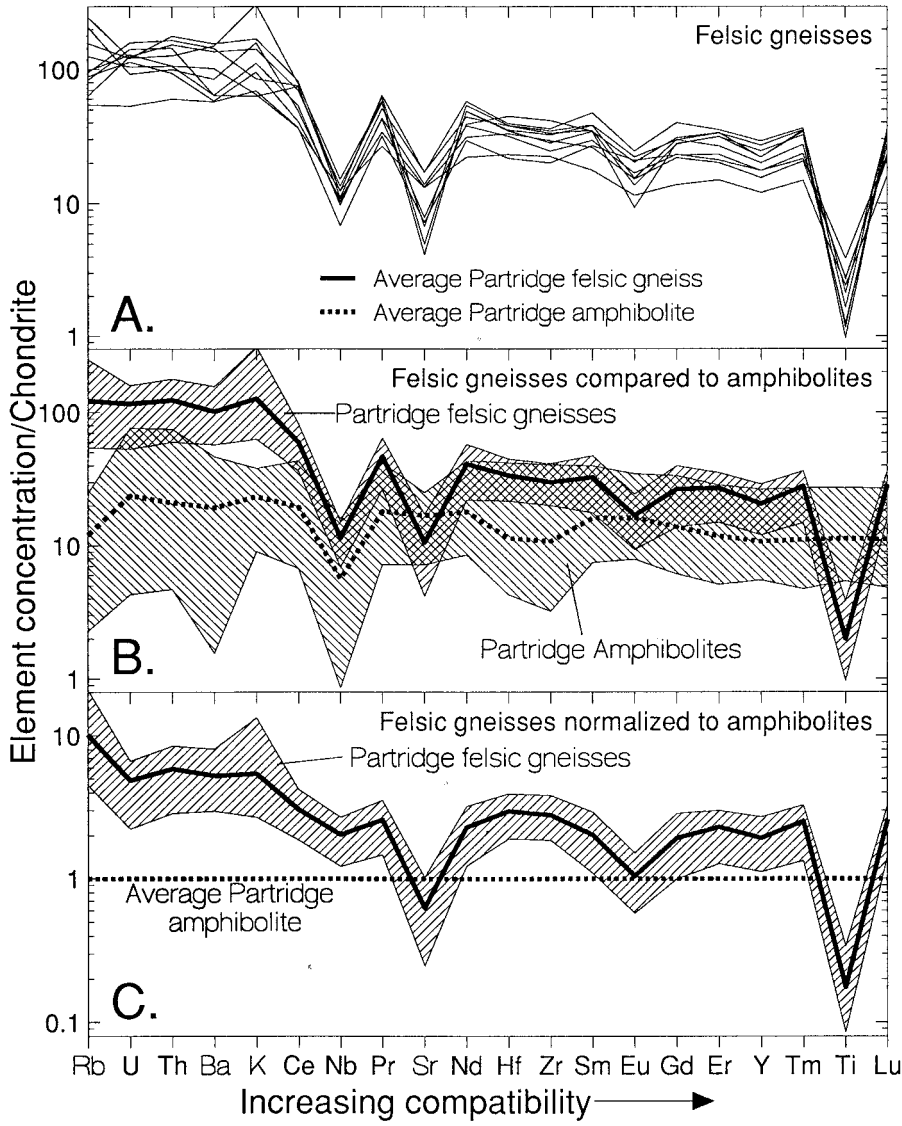

Fig. 11(A) Spider diagram showing the Partridge felsic gneisses. (B) Spider diagram comparing the range of patterns for the Partridge felsic gneisses compared to the Partridge amphibolites. Note that the felsic gneisses span a smaller range for all elements than do the amphibolites, except for K. (C) Spider diagram showing the range of values for the Partridge felsic gneisses normalized to the average Partridge amphibolite (presumed to be compositionally similar to the source rock for the Partridge felsic gneiss protolith magmas). The amphibolite average is calculated as in figure 9.

Nb anomalies are characteristic of felsic magmas in island arc environments but are less common elsewhere (Thompson and others, 1984). Figure 11B compares the Partridge felsic gneisses to the Partridge amphibolites. The felsic gneisses are clearly enriched in the less compatible elements with respect to the amphibolites, but, except for Ti, the more compatible elements in the felsic gneisses are similar in concentration to the amphibolites. The negative Nb anomaly is the only one the felsic gneisses generally share with the amphibolites. Figure 11C shows the range of the felsic gneiss compositions normalized to the average "unaltered" Partridge amphibolite. All elements are enriched in the felsic gneisses relative to the average amphibolite, except for Eu which is similar and Sr and Ti which are depleted. The negative anomalies for Sr, Eu, and Ti remain, but the Nb anomaly has nearly vanished.

TECTONIC SETTING

Numerous tectonic setting discriminant diagrams have been applied to the Ammonoosuc Volcanics. Although the data tend to scatter between several tectonic setting fields in these diagrams, it has been the conclusion of most workers (Aleinikoff, 1977; Shumway, ms; Leo, 1985, 1991; Schumacher, 1988) that the Ammonoosuc Volcanics best fit an island arc tectonic setting. Aleinikoff (1977) concluded that some of the Ammonoosuc amphibolites were erupted in an abyssal tholeiite (MORB) tectonic setting, and Shumway (ms) concluded that a back-arc basin setting was possible, largely on the basis of the bimodal distribution of compositions.

The tectonic setting discriminant diagrams applied in this study to the Partridge amphibolites include those of Pearce and Cann (1973), Pearce (1976, 1980, 1983), Pearce and Norry (1979), Wood (1980), Shervais (1982), Mullen (1983), and Meschede (1986), examples of which are shown in figure 12. In figure 12A (Ti-Zr-Y) the Partridge amphibolites form an elongate array spanning three fields occupied by low-K tholeiites (arcs), ocean floor basalts (MORB), and calc-alkaline basalts (one field contains only one sample). In a related diagram (Ti-Zr-Sr, not shown, Pearce and Cann, 1973), only one Partridge data point lies within the calc-alkaline field, and all other Partridge and Ammonoosuc amphibolites overlap the fields of ocean floor basalts (MORB) and low-K tholeiites (arcs). In this diagram the boundary between the calc-alkaline field and other fields has a nearly constant Ti/Zr ratio, so variations in Sr concentration due to alteration could not significantly add to the single sample in the calc-alkaline field. In figure 12B (Ti-V) the Partridge amphibolites span the island arc and MORB fields. In figure 12C (Nb-Zr-Y) all Partridge samples lie either in the field of N-MORB and arc basalts or in the field of arc basalts and some within-plate tholeiites (two samples only). In figure 12D (Ti-Zr) the Partridge amphibolites form an elongate array that overlaps the fields of arc lavas, within-plate lavas, and MORB. Many samples occur within the MORB field, and the array of data passes through and is nearly parallel to the MORB field.

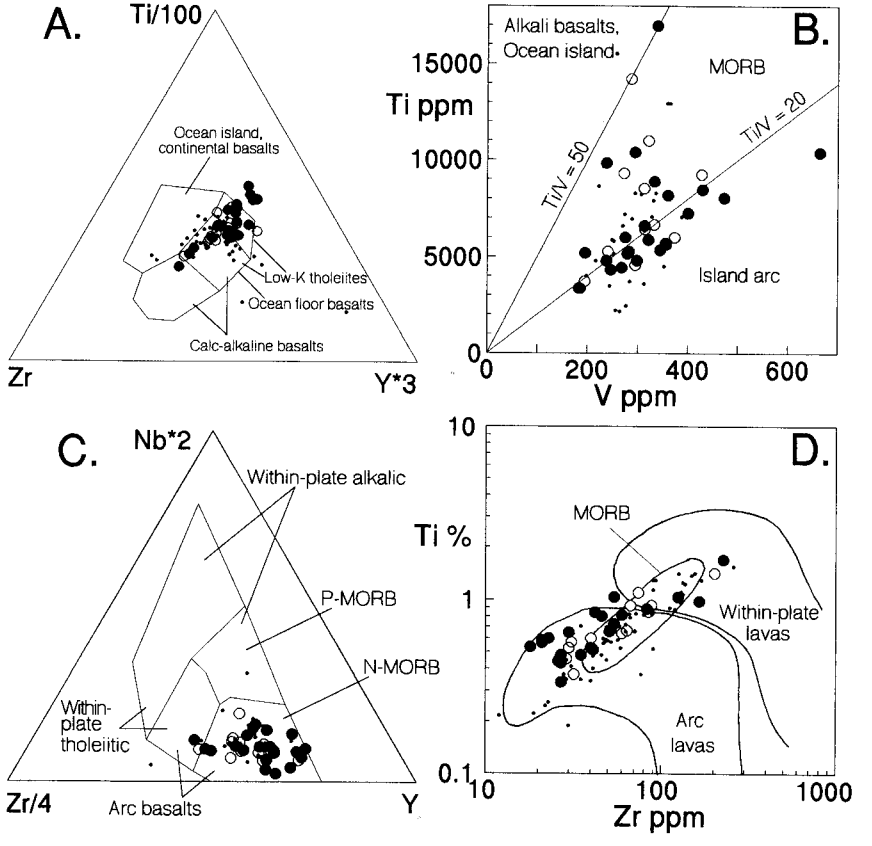

Fig. 12. Tectonic setting discriminant diagrams for Partridge Formation amphibolites showing Ammonoosuc Volcanics for comparison. (A) Ti–Zr–Y diagram after Pearce and Cann (1973). (B) Ti–V diagram after Shervais (1982). (C) Nb–Zr–Y diagram after Meschede (1986). (D) Ti–Zr diagram after Pearce (1980).

The tectonic setting discriminant diagrams indicate that the amphibolites have chemical similarities to MORB and tholeiitic island arc basalts, confirming comparisons made using REE and spider diagrams. Comparisons using REE and spider diagrams also indicate that the amphibolites have chemical similarities to back-arc basin basalts, which in some areas are transitional in composition between MORB and island arc basalts (Tarney, Saunders, and Weaver, 1977; Weaver and others, 1979; Hawkins and Melchior, 1985). To clarify the tectonic setting for the Partridge amphibolite protolith magmas, comparisons of the amphibolites to ocean ridge, back-arc basin, and island-arc basalts were made on chemical variation diagrams using the elements Cr, Ni, Ti, P, Ce, Y, Nb, and Zr (example in fig. 13). In figure 13, Partridge amphibolites can be distin-

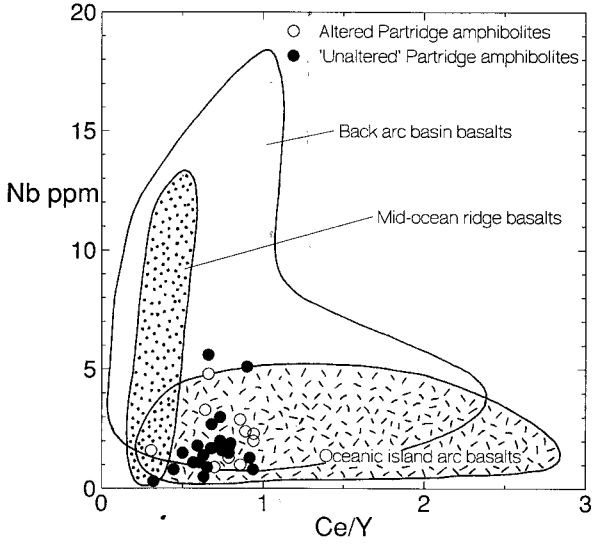

Fig. 13. Partridge amphibolites plotted with respect to the composition fields of mid-ocean ridge basalts, back-arc basin basalts, and basalts from oceanic island arcs. Data are from Lowder and Carmichael (1970), Tarney, Saunders, and Weaver (1977), Weaver and others (1979), Basaltic Volcanism Study Project (1981), Marcelot and others (1983), and Hawkins and Melchior (1985).

guished from normal MORBs on the basis of the lower Ce/Y ratios and generally higher Nb concentrations in MORB magmas. The Partridge amphibolites cannot be distinguished in figure 13 from tholeiitic-arc basalts or back-arc basin basalts, both of which overlap the field of Partridge data almost completely.

The major element compositions of felsic and mafic Partridge volcanics were compared with the ~36,000 igneous rock analyses in the PETROS geochemical database (Mutschler and others, 1981). In this comparison, each PETROS analysis was screened to exclude those having a sum of the 11 major oxides outside the range of 95 to 103 percent. The Partridge and accepted PETROS analyses were then normalized to 100 percent, with all Fe calculated as FeO. Each Partridge analysis was compared to each PETROS analysis, and each comparison ranked using a weighted least squares of the differences algorithm. The five PETROS analyses most similar to each Partridge sample were extracted and plotted on a global map. It is notable that 50 percent of the plotted analyses are in areas of Cretaceous to Recent island arc and back-arc basin environments, a proportion higher than the ~25 percent of such rocks in the database. Only 7 percent of the Partridge samples in this comparison were matched with ocean floor basalts, although such rocks make up ~10 percent of the database. Although the major elements are not particularly diagnostic, the results of this comparison also favor an

arc or back-arc tectonic setting for the Ammonoosuc Volcanics and volcanics in the Partridge Formation.

In figure 12 (and other figures not shown) it is difficult to distinguish between MORB and island-arc tectonic environments for the Partridge amphibolites. This may indicate that the mantle source for the Partridge and Ammonoosuc amphibolites was transitional between mantle sources typical of these environments. Basalts that are transitional between those from MORB and island-arc environments are common in back-arc basins (Hawkins, 1977; Hawkins and Melchior, 1985; Ikeda and Yuasa, 1989; Stern and others, 1990). Indeed, Shervais (1982) noted that back-arc basin basalts tend to span a wide range of Ti/V ratios, overlapping both island arc and MORB fields even for data from single basins. The wide range of Ti/V ratios in the Ordovician amphibolites (fig. 12B) and the overlapping of these rocks with MORB and island arc fields in various other discriminant diagrams suggest that these rocks are indeed transitional. Considering the evidence, it seems more likely that the protolith magmas for the Ordovician amphibolites were basalts erupted in a back-arc basin rather than the island-arc setting to which they are generally assigned.

The tectonic setting discriminant diagrams of Pearce, Harris, and Tindle (1984) have been applied to the Ammonoosuc felsic gneisses by Schumacher (1988), who concluded that an island arc setting was favored for these rocks. In figure 14 the Partridge felsic gneisses overlap the fields of Ammonoosuc samples but tend to plot at slightly higher Y and Y + Nb concentrations. In figure 14A the Partridge data straddle the boundary between the volcanic arc and syn-collision granite field and the field of ocean ridge granites. In figure 14B the Partridge felsic gneisses straddle the boundary between within-plate granites and volcanic arc granites.

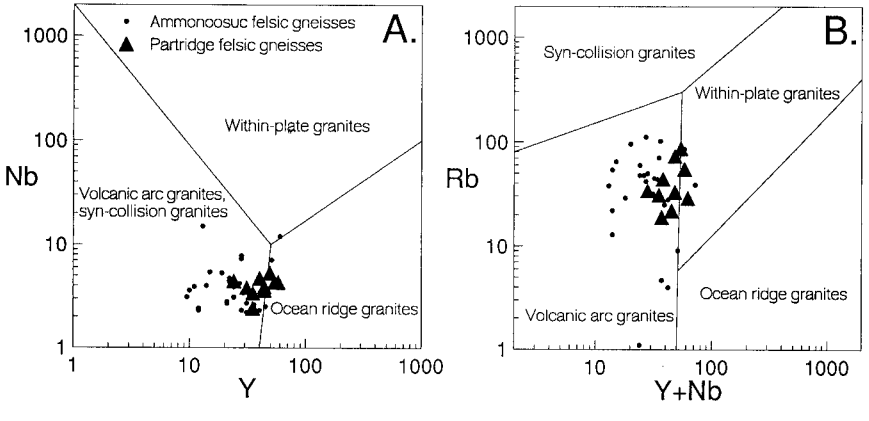

Fig. 14. Tectonic setting discriminant diagrams for Partridge Formation felsic gneisses, with felsic Ammonoosuc Volcanics shown for comparison (after Pearce, Harris, and Tindle, 1984).

Although a majority of the Partridge felsic gneisses plot in volcanic arc fields in figure 14, these diagrams imperfectly assign a tectonic setting in a way similar to the amphibolites. Although these tectonic setting discriminant diagrams are somewhat equivocal, they suggest that the felsic gneisses may at least be arc-related. Thus, and considering the fact that the felsic and mafic Partridge Volcanics are interbedded, a back-arc basin tectonic environment is favored for the Partridge and Ammonoosuc felsic gneisses.

A back-arc basin setting for the Ordovician volcanics is further supported by two additional points. First, bimodal volcanism is uncommon in island arc environments (Uyeda, 1977), although it is not unknown (Lowder and Carmichael, 1970; Bryan, Stice, and Ewart, 1972; Johnson and Arculus, 1978). Second, despite the similarity in age and spatial proximity of the dome gneisses and overlying Ordovician volcanics, lithologic comparison suggests that the dome gneisses are not genetically related to the Ordovician volcanics. Both the Ammonoosuc and Partridge volcanics are volumetrically dominated by tholeiitic mafic rocks in contrast to the dome gneisses which are dominated by calc-alkaline felsic rocks (Leo, Zartman, and Brookins, 1984; Leo, 1985, 1991). The dome gneisses do contain minor amounts of mafic rocks, but these are also calc-alkaline (Hollocher, 1988).

The evidence suggests that the Ordovician volcanics are not part of the Taconian arc proper, represented by Ordovician dome gneisses in the Bronson Hill anticlinorium, but instead represent an episode of back-arc spreading related to Taconian subduction beneath the arc. Back-arc volcanism is compositionally bimodal in some cases (Ikeda and Yuasa, 1989), and the overlap of the Ammonoosuc and Partridge amphibolites into MORB and island arc fields would be expected of the transitional magmas erupted in an area of incipient back-arc rifting (Shervais, 1982; Hawkins and Melchior, 1985; Ikeda and Yuasa, 1989; Stern and others, 1990).

ORIGIN OF THE AMPHIBOLITES

A variety of petrogenetic models were tested in an attempt to understand the genesis of the Partridge mafic volcanics and the nature of the Ordovician mantle source for these rocks. All models were run using the mineral/liquid partition coefficients in table 3. The most successful model, discussed here, involves continuous partial melting (Langmuir and others, 1977; Wood, 1979) which assumes continuous melting and liquid extraction while leaving a small volume (1 percent) of mechanically unextractable liquid in the residue. Although the interconnection of liquid-filled voids during melting may be a problem for models of this type (Maaløe, 1981), others conclude that such interconnection will occur at low proportions of melting and result in rapid liquid extraction (Ahern and Turcotte, 1979; Thompson and others, 1984; McKenzie, 1984; McKenzie and Bickle, 1988). Even if void interconnection is not spontaneous, dynamic recrystallization in the deforming mantle wedge may force

TABLE 3

Crystal/liquid partition coefficients for the models, and starting composition for the mantle source

	K	Ti	Rb	Sr	Y	Zr	Nb	Ba	La	Ce	Pr	Nd	Sm	Eu	Gd	Tb	Dy	Ho	Er	Tm	Yb	Lu	Hf	Th	U	Ni
Crystal/liquid partition coefficients for the basalt models*																										
Amphibole									0.18	0.23	0.31	0.43	0.62	0.74	0.77	0.78	0.74	0.69	0.64	0.59	0.54	0.49				
CPX	0.04	0.37	0.005	0.1	0.35	0.11	0.05	0.01	0.065	0.11	0.16	0.2	0.25	0.24	0.33	0.345	0.35	0.35	0.345	0.335	0.32	0.3	0.11	0.004	0.011	*
Garnet									0.005	0.02	0.05	0.08	0.24	0.3	0.6	0.9	1.4	2	2.8	4	6	9.3				
OPX	0.006	0.11	0.005	0.014	0.006	0.034	0.15	0.005	0.003	0.005	0.008	0.012	0.021	0.018	0.033	0.04	0.049	0.06	0.076	0.1	0.13	0.18	0.034	0.054	0.008	*
Plagioclase									0.13	0.12	0.11	0.1	0.085	0.5	0.075	0.07	0.065	0.061	0.058	0.057	0.056	0.055				
Spinel	0.0005	0.8	0.0003	0.0003	0.115	0.02	0.01	0.0003	0.03	0.033	0.036	0.041	0.05	0.045	0.07	0.085	0.105	0.115	0.12	0.115	0.106	0.09	0.02	0.02	0.02	7
Olivine	0.006	0.02	0.003	0.005	0.006	0.014	0.01	0.003	0.001	0.002	0.002	0.003	0.004	0.004	0.005	0.005	0.006	0.006	0.007	0.007	0.008	0.008	0.014	0.007	0.007	*
Chondritic mantle starting composition, ppm**																										
8	120	620	0.35	11	2	5.6	0.35	3.8	0.31	0.808	0.122	0.6	0.195	0.074	0.259	0.047	0.322	0.072	0.21	0.032	0.209	0.032	0.167	0.05	0.013	2200
Crystal/liquid partition coefficients for the dacite models***																										
Apatite	0	0.02	0.01	1.7	28	0.785	0.02	0.01	21	24	28	34	46	18	45	40	33	28	23	19	16	14	0.785	2	2	0.75
Biotite	5.6	1.5	3.3	0.12	0.12	0.9	1.8	0.44	0.034	0.037	0.04	0.044	0.058	0.145	0.075	0.085	0.1	0.12	0.15	0.17	0.18	0.185	0.9	1	0.1	10
CPX	0.037	0.4	0.02	0.27	1.9	1.545	0.6	0.076	0.2	0.45	0.7	0.95	1.35	0.82	1.7	1.85	1.9	1.9	1.85	1.8	1.7	1.6	1.545	0.5	0.1	21
Garnet									0.3	0.35	0.4	0.6	2.7	1.5	10.5	20	29	37	43	43	40	30				
Hornblende									0.5	0.85	1.3	1.8	3	3.1	4.5	5.5	6.2	6.7	6.7	6	5	4.3				
Ilmenite	0	250	0	0	0.06	0.575	5	0	0.005	0.005	0.005	0.01	0.01	0.01	0.02	0.03	0.05	0.06	0.07	0.08	0.09	1	0.575	0.43	0.06	10
Magnetite	0.01	9	0	0	0.13	0.75	2	0.01	0.03	0.04	0.05	0.06	0.08	0.09	0.1	0.11	0.12	0.13	0.14	0.16	0.18	0.2	0.75	1.6	0.5	17
Olivine	0.01	0.01	0.001	0.01	0.02	0.01	0.01	0.01	0.005	0.005	0.005	0.01	0.01	0.01	0.01	0.015	0.015	0.02	0.025	0.03	0.035	0.04	0.01	0.02	0.01	25
OPX	0.002	0.25	0.011	0.037	0.57	0.185	0.4	0.018	0.07	0.075	0.09	0.11	0.15	0.12	0.3	0.4	0.5	0.57	0.65	0.7	0.75	0.8	0.185	0.1	0.02	15
Plagioclase	0.15	0.05	0.04	2.3	0.077	0.168	0.04	0.29	0.21	0.19	0.17	0.152	0.121	1.4	0.1	0.09	0.083	0.077	0.07	0.063	0.058	0.051	0.168	0.04	0.11	0.04
Sphene									19	90	145	178	172	112	130	110	90	70	59	52	46	39				

* Values for Nb and U in spinel and Th in olivine were approximated; Ni values for olivine from the MgO-dependent equation of Hart and Davis (1978); Ni value for CPX from the olivine value times 0.25 (Conrad and Kay, 1984); Ni value for OPX from the olivine value times 0.4; MgO in olivine was assumed to vary with the liquid with an Mg-Fe exchange coefficient of 0.30 (Roeder and Emslie, 1970).

** Chondritic values: REE from Boynton (1984); Hf = Hf of Thompson and others (1984) * 0.82; others from Sun (1980). Ni value is for mantle rock, from the Basaltic Volcanism Study Project (1981, table 1.2.11).

*** Values for U in apatite, Ni in biotite, and Ni in ilmenite were approximated.

void interconnection and cause rapid melt extraction anyway. Model liquids accumulate in an otherwise static magma chamber and then undergo low pressure fractional crystallization. The mineral mode of the mantle source is assumed to be constant over the relatively small percentage of melting indicated by the models (3-15 percent). The initial mantle composition is assumed to be chondritic (table 3). An MgO concentration of 16 percent is calculated for all primary liquids, which is reasonable based on other studies (Nye and Reid, 1986; Basaltic Volcanism Study Project, 1981, chapter 1.4.2; Tatsumi, 1983), based on figures 1 and 2 of Irving (1978), and based on a melting temperature of about 1300°C (thermal models of Toksöz and Hsui, 1978; Tatsumi, 1983). The MgO and Ni concentrations in the model primary liquids do not vary significantly over the 3 to 15 percent melting range.

Although there is no unique solution for the mineralogy of the mantle source for the Partridge amphibolite protolith magmas, there are several constraints. Assuming an initial range of simple REE patterns for the source (flat, LREE-enriched, LREE-depleted), preliminary models showed that the best results are obtained if the restite did not contain amphibole (produces MREE-depleted patterns), plagioclase (produces a negative Eu anomaly), or garnet (produces sharp HREE depletion). Maximum limits on these phases, based on inspection of model REE patterns, are 3 percent for amphibole, 1 percent for plagioclase, and 0.1 percent for garnet. As these percentages are small, amphibole, plagioclase, and garnet were not used in the model presented below. Apatite in the restite can be excluded since apatite-saturated basalt liquid would have several wt percent P_2O_5 (Watson, 1979; Ryerson and Watson, 1987), which is not seen. Rutile, ilmenite, sphene, and other Ti-rich phases in the restite can be eliminated since basalt liquids with these phases would contain several wt percent TiO_2 (Green and Pearson, 1986). At high pressure, phlogopite-saturated basaltic liquids have several wt percent K_2O (Tatsumi and Koyaguchi, 1989; Edgar, 1987), which is also not seen in the Partridge amphibolites (except in sample 12A which has a high K_2O content because of alteration, as described above).

With the elimination of garnet, plagioclase, amphibole, phlogopite, apatite, and Ti-rich phases from the mantle source rock, the remaining minerals likely to have been present are olivine, orthopyroxene, clinopyroxene, and spinel. These phases are consistent with the models discussed below and with current understanding of upper mantle petrology. The mineral mode used in the model described here is 68 percent olivine, 20 percent orthopyroxene, 10 percent clinopyroxene, and 2 percent spinel. This mode is within the range of several spinel lherzolites having flat and LREE-depleted REE patterns and Lu concentrations in the range of 1x to 2x chondrites (Basaltic Volcanism Study Project, 1981, text and table 1.2.11.5). The model liquid compositions are not very sensitive to variations in the mantle mode for the four included phases.

Melting lherzolite at high pressure yields liquids that are rich in the olivine component with respect to multiply saturated low pressure liqui-

dus surfaces (Grove and Kinzler, 1986). Since decreasing pressure associated with the rise of basaltic magma toward the surface results in expansion of the olivine liquidus stability field, the primary liquids initially fractionate olivine. On this basis an initial set of liquids was calculated involving fractional crystallization of olivine from the primary model liquids. Comparison of the norms of the "unaltered" Partridge amphibolites with low-pressure basalt liquidus fields (Longhi, 1991) along with principal component analysis indicates that the major element compositions of these rocks were controlled by fractionation or accumulation of olivine (± orthopyroxene), augite, and plagioclase in proportions of approx 60:20:20. On this basis a second set of liquids was calculated assuming that 3-phase cocrystallization began at about 150 ppm Ni and 10 percent MgO, which is the composition of the most Ni- and MgO-rich Partridge amphibolites that are not thought to be altered or to contain accumulated olivine (Hollocher, 1985b). Model liquids have this composition after about 13 percent olivine fractionation from the primary liquid.

The primary model liquids have ~394 ppm Ni, ~16 percent MgO, and $Mg/(Mg + Fe^{2+})$ (Mg′) of 0.75. In figure 15A, Lu/Ce ratios and Ce concentrations change markedly with proportion of melting to form an array of primary model liquids. The primary liquid array shown extends from 3 to 15 percent melting and includes the Lu/Ce ratios of most samples. Fractional crystallization from 0 to 50 percent is shown from the model primary liquids, causing an increase in Ce concentrations with increasing degree of crystallization. The liquid Lu/Ce ratio changes little during fractionation, and both olivine-only and multiple phase crystallization produce fractionation lines that are nearly coincident in figure 15. Samples 7 and 22A lie in the field of LREE-depleted rocks and cannot have been derived from a chondritic mantle by the two-stage model presented here. These samples must instead have been derived from a previously LREE-depleted source. Although sample 6 can be derived from a chondritic mantle source at very large proportions of melting (~80 percent), this is unreasonable, and sample 6 is probably also derived from a somewhat LREE-depleted source. Sample 21 cannot be reached by model liquids after only 50 percent crystal fractionation but can be explained by either 70 to 80 percent crystal fractionation of the model liquids shown or less fractionation of liquids derived from a more REE-enriched source. Six samples lie at lower Ce concentrations than the primary liquid curve, and these may have been derived from a mantle source having chondritic REE ratios but less than chondritic REE concentrations. In figure 15 B and C olivine crystallization rapidly reduces Ni, MgO, and Mg′ values, and the evolved model liquids closely follow the field of "unaltered" Partridge amphibolite data.

Figure 16A shows the range of REE patterns for the Partridge amphibolites compared to several model liquids. Primary liquids derived from 3, 6, and 10 percent melting (thick solid black lines) mimic the straight, slightly LREE-enriched slopes and slight positive Eu anomalies

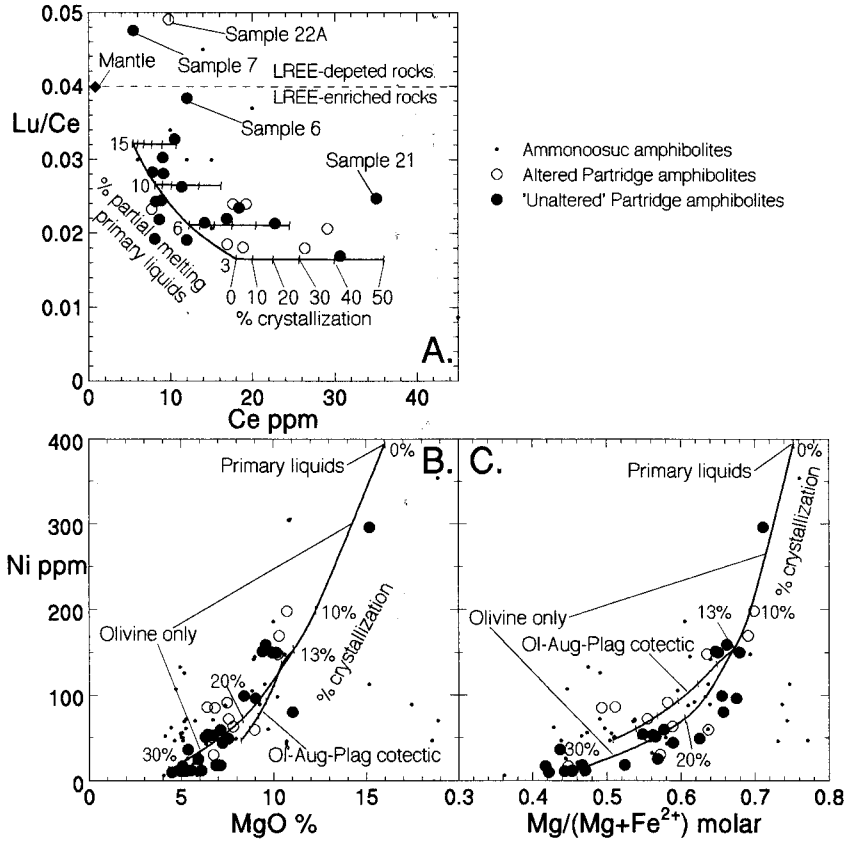

Fig. 15. Diagrams showing the results of a mathematical model to generate the protolith magmas for the Partridge amphibolites. (A) This diagram shows that most samples are modeled successfully by 3 to 15 percent melting of a chondritic mantle source producing a range of primary liquids, which then fractionate to produce a field of evolved liquids that encompasses most Partridge amphibolites. The 0 to 50 percent range of fractional crystallization does not differentiate between olivine only and cocrystallization of an olivine + plagioclase + augite assemblage since the fractionation curves are nearly coincident. (B) Model magma compositions shown with respect to the compatible components Ni and MgO. The primary liquids evolve by fractional crystallization along two paths, shown for comparison. Zero to 30 percent olivine crystallization extends along the complete range of Partridge data. Cocrystallization of an olivine + plagioclase + augite assemblage, starting after 13 percent olivine crystallization, extends crystallization an additional 50 percent. (C) Model magma compositions shown with respect to the components Ni and Mg/(Mg + Fe^{2+}). As in 15B, the path of 0 to 30 percent olivine crystallization matches the range of Partridge amphibolite data well. The olivine + plagioclase + augite cocrystallization path also follows the field of Partridge amphibolite data. (B) and (C) show only one set of model curves since all are nearly coincident for the 3 to 15 percent melting shown.

found in most Partridge amphibolites. Model liquids derived from the primary liquids by 30 percent olivine crystallization (dotted lines) are also very similar to Partridge amphibolites. One model liquid shown was derived from 13 percent olivine fractionation followed by 37 percent

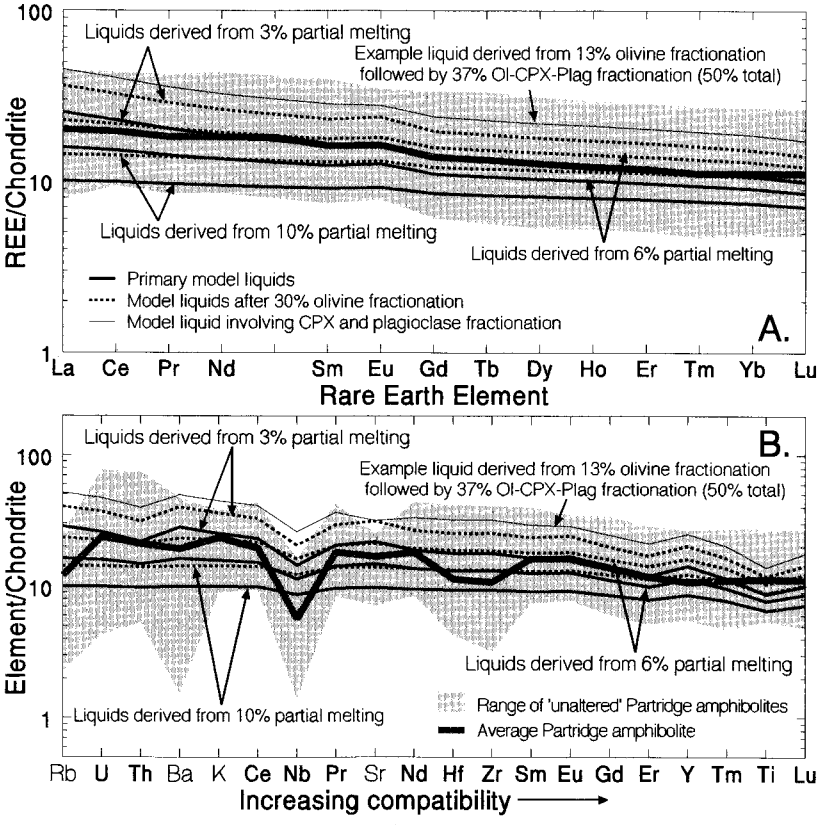

Fig. 16. REE diagram (A) and spider diagram (B) showing the range and average of Partridge amphibolites compared to example model liquid compositions for 3, 6, and 10 percent melting, each followed by 0 or 30 percent olivine crystallization. One curve in each diagram is shown for liquid from 3 percent partial melting followed by 13 percent olivine fractionation and then by 37 percent cocrystallization of an olivine + plagioclase + augite assemblage to total 50 percent crystallization.

cofractionation of olivine, augite, and plagioclase as described above (total 50 percent, thin black line). The shape of this curve does not differ significantly from the others.

Figure 16B is a spider diagram showing the range of incompatible element patterns for the Partridge amphibolites compared to the same model liquids as in figure 16A. The general shape of the average amphibolite (elements U, Th, Ba, K, Ce, Pr, Sr, Nd, Sm, Eu, Gd, Er, Y, Tm, Lu) is modeled well by the primary liquids derived from 3 to 6 percent melting and including olivine fractionation. Except for the formation of a small negative Sr anomaly, the pattern shape does not change significantly in the example fractionated liquid derived from 13 percent olivine crystallization and 37 percent cocrystallization. Note that

a small negative Nb anomaly is present in these model liquids as is a small negative Ti anomaly.

The REE patterns, small positive Eu anomalies, most elements in the spider diagrams, and Ni, Mg, and Mg′ in the amphibolites are matched closely by the model liquids. These indicate that the protolith magmas for most amphibolites were produced by 3 to 15 percent melting of a chondritic spinel lherzolite mantle source, followed by modest percentages of fractional crystallization of olivine ± plagioclase ± augite. Although generally successful, some elements are not closely modeled. Ignoring the mobile elements, the model fails to account for the large negative anomaly for Nb, the small negative Hf and Zr anomalies (except in samples 14A, 21, 23, 32), and the lack of a negative Ti anomaly found in the Partridge amphibolites. Large negative Nb anomalies and small negative Hf and Zr anomalies, as mentioned above, are characteristic of island-arc and some back-arc basin basalts. The origin of these anomalies in modern volcanics is still unclear, but they are probably inherited from the mantle sources. The negative Ti anomaly in the model liquids is common, though not universal, in island-arc and back-arc basin basalts. Its absence in the Partridge amphibolites may reflect a mantle source slightly enriched in Ti. As described above, samples 7, 22A, and possibly 6 must have been derived from a LREE-depleted source rather than the chondritic source used in the model described here. The model results clearly require inhomogeneity in the mantle source region from which the suite of amphibolite protolith magmas came.

ORIGIN OF THE PARTRIDGE FELSIC GNEISSES

The bimodal distribution of the Ammonoosuc and Partridge volcanics (fig. 2) indicates that the mafic and felsic rocks were not derived by a continuous process. If this were the case, intermediate magmas would be plentiful, and no composition gap would exist.

Plots of Partridge felsic gneiss norms in the quaternary quartz–albite–orthoclase–anorthite liquidus system (Winkler, 1979; not shown) indicate that all samples but one plot within the stability fields of quartz and plagioclase near the 5 kb P_{H20} quartz-plagioclase cotectic surface. These results are similar to those for the felsic Ammonoosuc Volcanics (Leo, Zartman, and Brookins, 1984; Leo, 1991; Schumacher, 1988), although the felsic rocks from the upper member of the Ammonoosuc are typically higher in K_2O than felsic rocks in the Partridge. The apparent rarity of K-feldspar on the liquidus of Ammonoosuc and Partridge felsic rocks and the low K_2O contents of most of these rocks indicate that they were not derived by partial melting of granitic or pelitic sedimentary material but rather were derived from more mafic rocks. Experimental studies show that quartz-normative, peraluminous, low- to medium-K dacitic and rhyolitic liquids can be derived from the partial melting of basaltic materials under a variety of P-T-a_{H20} conditions with pyroxenes and/or amphibole left in the restite (Helz, 1976; Spulber and Rutherford, 1983; Ellis and Thompson, 1986; Hacker, 1990). On these bases a variety of

models were tested involving the partial melting of basaltic rocks in the deep crust to generate the protolith magmas for the Partridge felsic gneisses.

The models are based on the assumption that the region of melting was composed largely of mafic lavas and intrusives having compositions similar to the Partridge and Ammonoosuc amphibolites. This assumption is reasonable considering that the large negative Nb anomaly in the Partridge felsic gneisses strongly indicates a Nb-depleted source rock similar to these amphibolites. Consistent with the lack of involvement of felsic continental crust during melting is the lack of inheritance in zircons from the Ammonoosuc and Partridge felsic gneisses (Tucker and Robinson, 1990).

A variety of models were made to test the possibility of the presence of sphene, rutile, amphibole, garnet, and biotite in the restite or fractionating assemblage. Except for biotite, all but insignificant quantities of these phases result in poorer model fits for the REEs, so these phases were omitted. Biotite cannot be excluded on this basis, but its survival in the restite is unlikely considering the low-K composition of the model source and the relatively K-rich model liquids extracted from it. In any case, small quantities of biotite do not significantly affect the model liquid compositions so it was omitted as well. Lacking other constraints, the average amphibolite (caption of fig. 9) was used for the source composition, and its norm used for the source assemblage and mineral proportions (plagioclase 52.85 percent, CPX 14.48 percent, olivine 4.37 percent, orthopyroxene 21.93 percent, ilmenite 2.26 percent, magnetite 1.82 percent, apatite 0.32 percent). As a crustal metamorphic rock this norm represents a plagioclase + pyroxene + olivine granulite.

The most successful model, presented here, involves two stages: 10 percent equilibrium melting of the mafic source rock, followed by fractional crystallization of the resulting liquid. Equilibrium melting was chosen over the continuous melting mechanism used in the mafic rock model, because the much higher viscosity of felsic liquids would inhibit rapid restite-liquid separation. Although model liquids derived from 10 percent melting give a reasonably good match to the Partridge felsic gneisses, a 20 percent fractional crystallization stage is required to reproduce the low Cr and Ni concentrations present in most of the felsic gneisses. The fractionating mineral mode was chosen to be identical to the restite mode, as there are no other constraints.

Figure 17A shows the model results for the REEs in comparison to the average Partridge amphibolite (the model source) and the range of felsic gneiss compositions. The model liquids derived from 10 percent melting match the LREEs and the negative Eu anomaly in the average felsic gneisses. The HREEs in the model liquids are low with respect to the average Partridge felsic gneisses by a factor of about 1.5, but the model liquid closely matches several individual samples. The model liquid from 10 percent melting has 26 ppm Cr and 10 ppm Ni, similar to sample 45 but substantially higher than the median values of 2 ppm Cr

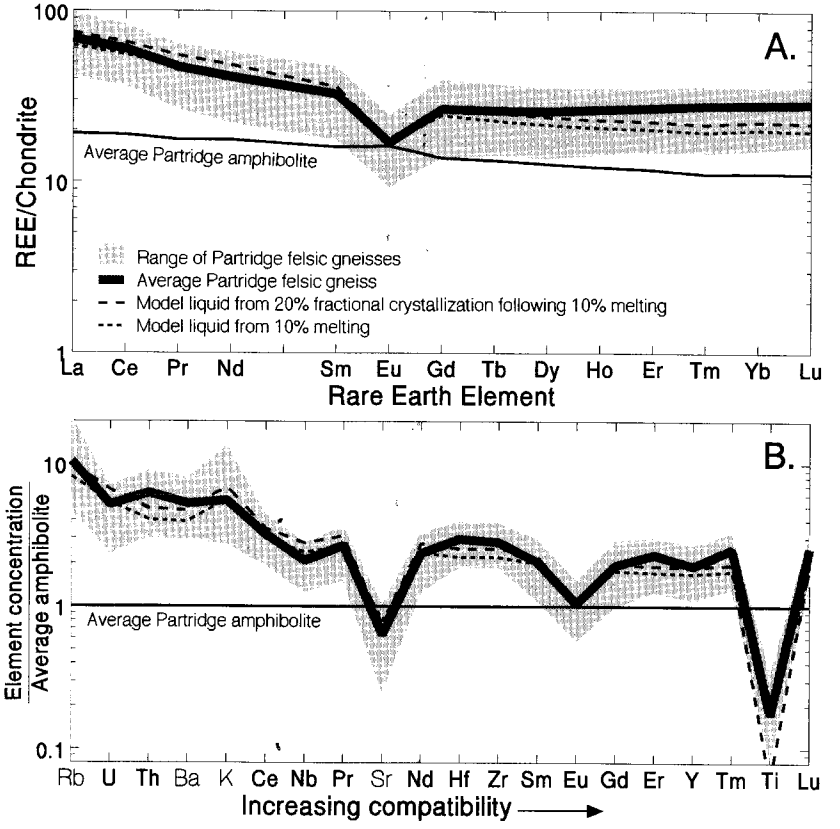

Fig. 17(A) REE diagram showing the range and average of Partridge felsic gneisses compared to the average LREE-enriched amphibolite (caption of fig. 8) and model liquids generated from a pyroxene granulite source by 10 percent partial melting followed by 20 percent fractional crystallization. (B) Spider diagram showing the range and average of Partridge felsic gneisses normalized to the average amphibolite (caption of fig. 9, the composition of the presumed source rock). Also shown are the compositions of the same model liquids as in figure 17A.

and 4 ppm Ni. Twenty percent fractional crystallization reduces the Cr and Ni concentrations in the model liquid to 4 and 2 ppm, respectively, and improves the model fit for the HREE slightly.

Figure 17B shows the model results in comparison to the felsic gneisses on a spider diagram, normalized to the average Partridge amphibolite (the model source). The general negative slope of the Partridge felsic gneisses is modeled well as are the large negative anomalies derived from plagioclase (Sr, Eu) and Fe-Ti oxides (Ti) in the restite and fractionating assemblage. Even the small positive K and Rb and

negative Nb anomalies present in the model liquids have their counterparts in the felsic gneisses. The difference between the fractionated model liquid and the average Partridge felsic gneiss is less than a factor of 1.5 for most elements, Ti is within a factor of three, and Cr and Ni concentrations are within a factor of two. However, considering the uncertainties in the assumptions of the model and the possibility of post-eruptive alteration processes, the match between the model liquid and the felsic gneisses is remarkably good. The good fit indicates that the model is reasonable and confirms the results of similar models calculated for the Ammonoosuc felsic gneisses (Schumacher, 1988).

CONCLUSIONS

The Ammonoosuc Volcanics and volcanics in the Partridge Formation in west-central Massachusetts are mineralogically and chemically similar and can be considered to be parts of the same volcanic series. Conclusions for the Partridge volcanics can therefore be applied to the Ammonoosuc Volcanics. Volcanics in these two units can, with present understanding, be discriminated only on the basis of field associations that include the internal stratigraphy of the Ammonoosuc Volcanics and the interbedding of volcanics in the Partridge Formation with sulfidic mica schist.

The Partridge amphibolites appear to form a single chemical group that is most similar to tholeiitic basalts. The amphibolites are characterized by straight, slightly LREE-enriched patterns with MREE concentrations of about 7x to 35x chondrites, and most have small positive Eu anomalies. Two samples are slightly LREE-depleted. Small negative Hf and Zr anomalies and large negative Nb anomalies also occur. The Partridge felsic gneisses have chemical compositions similar to calc-alkaline dacites, rhyodacites, and rhyolites. The felsic gneisses are somewhat LREE-enriched with La concentrations of 40x to 100x chondrites and MREE and HREE concentrations of 15x to 40x chondrites. All felsic gneisses have negative anomalies for Eu, Sr, Nb, and Ti. With respect to the mafic rocks, the felsic rocks are enriched in most incompatible elements but are depleted in Ti and Sr and have similar Eu concentrations.

Geochemical modeling was carried out to understand better the origin of the Partridge amphibolites and the nature of the mantle source regions. The models indicate that the mantle source for most of the Partridge amphibolites was a spinel lherzolite having approximately chondritic concentrations of most incompatible elements but depleted in Nb by a factor of ~3. The source for most amphibolites was also depleted in Hf and Zr by factors of about ~1.6. The mantle source region was clearly inhomogeneous, with the sources for four of the 35 Partridge amphibolites having had no depletion in Hf and Zr, and with LREE-depleted sources being required for two and possibly three amphibolites.

Modeling suggests that the primary liquids were derived from the mantle source by 3 to 15 percent melting, followed by a minimum of 13 percent fractionation of olivine with subsequent fractionation of olivine (±orthopyroxene) ± plagioclase ± augite.

Geochemical modeling was carried out for the Partridge felsic gneisses to constrain better their origins and the nature of their source regions. The models indicate that the protolith magmas were probably derived by partial melting of basaltic material, probably as a plagioclase + pyroxene + olivine granulite in the lower crust. The models indicate that the source composition was already depleted in Nb, supporting the assumption that the region of melting was made of rock similar in composition to the Partridge amphibolites. The models indicate that the Partridge felsic gneisses were derived from the pyroxene granulite source region by 10 percent melting followed by about 20 percent fractional crystallization.

The success of the geochemical models for both the amphibolites and felsic gneisses is remarkable, considering that both have experienced sillimanite grade regional metamorphism. The success of the models is also remarkable considering the many assumptions that had to be made. Many of the constraints used to model modern volcanics, such as igneous mineralogy, assured igneous chemical composition, and obvious eruptive environment, no longer exist for these ancient rocks.

The tectonic environment for eruption of the protolith magmas for the Ammonoosuc Volcanics and volcanics in the Partridge Formation is based on tectonic setting discriminant diagrams, comparisons with major element analyses in the PETROS geochemical database, chemical comparisons with modern volcanics, and lithologic comparisons with the Ordovician dome gneisses in the Bronson Hill anticlinorium with which the Ordovician volcanics are presently associated. The Ordovician volcanics are here interpreted as having erupted in an early episode of back-arc spreading related to subduction beneath Taconian arc. The Lawrence Head Volcanics in Newfoundland, of upper Middle Ordovician age, have also been interpreted to have erupted in a back-arc basin related to the Taconian island arc (Pickering, 1987). These submarine volcanics form a unit about 800 m thick, similar to the thickness of the Ordovician volcanics in west-central Massachusetts.

A back-arc basin tectonic setting for the Ordovician volcanics raises two principal problems. First, the Silurian-Devonian stratigraphy that overlies the Partridge Formation is thin in the Bronson Hill anticlinorium compared to much thicker units of similar age in the Merrimack synclinorium to the east (Thompson, ms). If the Ammonoosuc and Partridge volcanic series developed in an extensional basin, why should the Silurian-Devonian sequence above them be thin? The Silurian and Devonian units that overlie the Ammonoosuc Volcanics and Partridge Formation rest on an unconformity, indicating that the hypothetical Ordovician back-arc basin was uplifted and eroded prior to Silurian deposition.

The second problem is a question of proximity. If the Ordovician dome gneisses in the Bronson Hill anticlinorium represent the Taconian magmatic arc, and if the Ordovician volcanics were erupted in a back-arc basin, how did the volcanics become placed structurally above them? This brings up the problem of the nature of the contact between the Ammonoosuc Volcanics and the underlying dome gneisses, a point of continuing debate despite extensive study. Evidence where the units are well mapped in Massachusetts and southwestern New Hampshire suggests that the contact is depositional, probably an unconformity (Schumacher, 1988). Leo (1985, 1991) working principally in central and northern New Hampshire believes the dome gneisses and Ammonoosuc Volcanics to be cogenetic and to be in intrusive contact. The age overlap between the Ordovician volcanics and underlying dome gneisses is consistent with this interpretation (Zartman and Leo, 1985; Tucker and Robinson, 1990). Geochemical and mineralogical comparisons, however, suggest that the dome gneisses and the Ordovician volcanics are not cogenetic (Hollocher and Lent, 1987; Hollocher, 1988). To answer the question of proximity, the interpretation here that the Ordovician volcanics were erupted in a back-arc basin requires that the volcanics and the underlying dome gneisses be in contact along a fault. Robinson, Tucker, and Hollocher (1989) suggested that the contact may be an intra-arc extensional fault that developed while the arc was active. Intra-arc extensional faulting is common in modern island arcs, and thrust faulting in arc environments has also been described even to the extent of placing back-arc basin volcanics over the arc (Hawkins and others, 1984). Work on the metamorphic history of the Ammonoosuc Volcanics and adjacent dome gneiss in New Hampshire (Kohn, 1991, and oral communication) suggests that the two presently adjacent units experienced distinctly different early Acadian metamorphic conditions, implying that the two units were juxtaposed along a synmetamorphic fault. This suggestion is supported by the observation that the Ammonoosuc-dome gneiss contact commonly appears to be a region of high strain.

ACKNOWLEDGMENTS

I would like to thank Peter Robinson for his help in the early years of this project. I thank Howard Jaffe, J. Michael Rhodes, and Earl J. McWhorter for their reviews of an early version of this manuscript. I particularly thank Ray Coish, Sorena Sorensen, Peter Robinson, and John Schumacher for their thorough reviews that have greatly improved this manuscript. I thank Barbara Hancher for her help preparing and analyzing samples for REE, Hf, Th, and U, and for data entry. Sample collection and XRF analyses were supported by NSF grants EAR-8116197 to Peter Robinson and J. Michael Rhodes, and EAR-8410370 to Robinson. ICPMS analyses were made possible by NSF grant USE-8950970 to Kurt Hollocher and George Shaw.

APPENDIX 1

Analytical Techniques

One to ten kilogram samples of rock were hand crushed to 0.5 to 1 cm size using a steel hammer on a wood block or with a steel-tooth hydraulic splitter. Fines, pieces containing joints, veins, metal scrapings, or weathered parts were discarded. Suitable chips were cleaned by two stages of vigorous shaking with deionized water in a closed polyethylene container, with the abraded fines being discarded. About 250 g of the air-dried chips were crushed to a fine powder in a 15 cm Spex tungsten carbide shatterbox for about 150 sec. Contamination from the grinding vessel was determined to be negligible for all analyzed elements, including Nb.

All XRF analyses were made in duplicate at the Department of Geology and Geography X-Ray Laboratory, University of Massachusetts, Amherst. Major elements (Si, Ti, Al, Fe, Mn, Mg, Ca, K, P) were analyzed using the fused glass disk method with a chromium X-ray tube. Trace elements were analyzed using pressed powder pellets and a molybdenum tube (Y, Sr, Rb, Pb, Ga, Th) or a gold tube (Nb, Zr, Zn, Ni, Cr, V, La, Ce, Ba). Na was analyzed by flame photometry using a lithium internal standard and unflavored Jell-O® as a wetting agent. FeO was determined by titration, and Fe_2O_3 determined by difference. Na_2O, FeO, and Fe_2O_3 were corrected for loss on ignition to put them on the same anhydrous basis as the other major elements.

TABLE 4

Standard concentrations, detection limits, and analytical precision for ICP-MS analyses

Element	Analyzed Isotope	NBS-688* basalt	NBS-278* obsidian	Detection Limits**	Analytical Precision*** NBS-688	NBS-278
La	139	4.74 ppm	31.93 ppm	0.36 ppm	25%	2%
Ce	140	11.92 ppm	63.02 ppm	0.05 ppm	2%	2%
Pr	141	1.73 ppm	7.08 ppm	0.04 ppm	2%	2%
Nd	146	8.16 ppm	27.00 ppm	0.04 ppm	2%	2%
Sm	152	2.44 ppm	5.73 ppm	0.03 ppm	2%	2%
Eu	151	1.01 ppm	0.81 ppm	0.03 ppm	2%	2%
Gd	158	2.90 ppm	5.49 ppm	0.03 ppm	2%	2%
Tb	159	0.50 ppm	0.97 ppm	0.03 ppm	2%	2%
Dy	163	3.27 ppm	6.26 ppm	0.03 ppm	2%	2%
Ho	165	0.71 ppm	1.36 ppm	0.03 ppm	2%	2%
Er	166	2.04 ppm	4.07 ppm	0.03 ppm	2%	2%
Tm	169	0.31 ppm	0.65 ppm	0.03 ppm	2%	2%
Yb	174	2.01 ppm	4.41 ppm	0.03 ppm	2%	2%
Lu	175	0.31 ppm	0.70 ppm	0.03 ppm	2%	2%
Hf	178	1.60 ppm	8.40 ppm	0.07 ppm	2%	2%
Th	232	0.46 ppm	12.40 ppm	0.05 ppm	7%	2%
U	238	0.37 ppm	4.58 ppm	0.01 ppm	18%	4%

* Compiled from literature values and unpublished standard addition analyses of Hollocher; REE values smoothed according to the chondrite normalizing factors of Boynton (1984).

** Twice the standard deviation of the blanks.

*** One standard deviation, based on standards run at the beginning and end of analytical runs, and then calculated as unknowns using the run calibration curves.

Analyses of the REE, Hf, Th, and U were made using a VG Instruments PQ2+ ICPMS instrument at the Union College Geology Department. ICPMS analyses for La, Ce, and Th supersede XRF values in table 1. Samples, standards, and blanks were prepared identically. Rock powders were dried in silica glass crucibles at 110°C for 2 hrs, and Johnson-Mathey $LiBO_2$ flux (Grade 1, Batch S97378) was dried in a ceramic crucible at 600°C overnight. 0.1000 ± 0.0002 g of rock powder was weighed and mixed in a small glass vial with 0.6000 ± 0.0010 g of $LiBO_2$ flux. The samples were fused in high-purity graphite crucibles at 980°C for a total of 9 min, with the molten contents briefly swirled at 3 min intervals. The molten bead was poured into 100 ml of 7 percent high-purity HNO_3 and stirred until dissolved (about 5 min). No undissolved material except graphite was ever observed. This solution was diluted by a factor of 10 and mixed with internal standards for analysis. The REEs were analyzed using 200 ppb (in solution) of Cs and Ta as internal standards. Hf, Th, and U were analyzed using 200 ppb of Lu and Bi as internal standards. NIST-688 basalt and NIST-278 rhyolite obsidian were used as concentration standards (accepted compositions given in table 4).

ICPMS operating conditions included a sample pumping rate of 0.8 ml/min, a nebulizer argon flow of 0.86 l pm, an auxiliary argon flow of 0.6 l pm, a cooling argon flow of 13 l pm, an induction coil power of 1350 W, and reflected power of about 2 W. Sensitivity was about 3×10^6 cps/ppm (in solution) for ^{133}Cs. Blank count rates for most elements were 20 to 30 cps, except for ^{140}Ce (150 cps) and ^{139}La (1200 cps) due to contamination from the $LiBO_2$ flux. Raw counts were corrected for detector dead time, background, and oxide and hydroxide interferences ($CeO^+/Ce^+ \approx 0.02$). Standard calibration curves were calculated using the blanks and standards analyzed at the beginning and end of each analytical run.

References

Ahern, J. L., and Turcotte, D. L., 1979, Magma migration beneath an ocean ridge: Earth and Planetary Science Letters, v. 45, p. 115–122.

Aleinikoff, J. N., 1977, Petrochemistry and tectonic origin of the Ammonoosuc Volcanics, New Hampshire-Vermont: Geological Society of America, v. 88, p. 1546–1552.

Arculus, R. J., 1976, Geology and geochemistry of the alkali basalt-andesite association of Grenada, Lesser Antilles island arc: Geological Society of America Bulletin, v. 87, p. 612–624.

Basaltic Volcanism Study Project, 1981, Basaltic Volcanism on the Terrestrial Planets: New York, Pergamon Press, Inc., 1286 p.

Bice, D. C., 1985, Quaternary volcanic stratigraphy of Managua, Nicaragua: correlation and source assignment for multiple overlapping plinian deposits: Geological Society of America Bulletin, v. 96, p. 553–566.

Billings, M. P., 1937, Regional metamorphism of the Littleton-Moosilauke area, New Hampshire: Geological Society of America Bulletin, v. 46, p. 463–566.

Box, S. E., and Patton, W. W., Jr., 1989, Igneous history of the Koyukuk terrane, western Alaska: constraints on the origin, evolution, and ultimate collision of an accreted island arc terrane: Journal of Geophysical Research, v. 94, no. B11, p. 15843–15867.

Boynton, W. V., 1984, Cosmochemistry of the rare earth elements: Meteorite studies, *in* Henderson, P., editor, Rare Earth Element Geochemistry: Amsterdam, Elsevier, p. 63–114.

Briqueu, Louis, Bougault, H., and Joron, J. L., 1984, Quantification of Nb, Ta, Ti and V anomalies in magmas associated with subduction zones: petrogenetic implications: Earth and Planetary Science Letters, v. 68, p. 279–308.

Bryan, W. B., Stice, G. D., and Ewart, A., 1972, Geology, petrography, and geochemistry of the volcanic islands of Tonga: Journal of Geological Research, v. 77, p. 1566–1585.

Conrad, W. K., and Kay, R. W., 1984, Ultramafic inclusions from Adak Island: crystallization history and implications for the nature of primary magmas and crystal evolution in the Aleutian arc: Journal of Petrology, v. 25, p. 88–125.

Dixon, T. H., and Stern, R. J., 1983, Petrology, chemistry, and isotopic composition of submarine volcanoes in the southern Mariana arc: Geological Society of America Bulletin, v. 94, p. 1159–1172.

Edgar, A. D., 1987, The genesis of alkaline magmas with emphasis on their source regions: inferences from experimental studies, *in* Fitton, J. G., and Upton, B. G. J., editors, Alkaline Igneous Rocks: Geological Society (London) Special Publication 30, p. 29–52.

Ellis, D. J., and Thompson, A. B., 1986, Subsolidus and partial melting reactions in the quartz-excess CaO + MgO + Al_2O_3 + SiO_2 + H_2O system under water-excess and water-deficient conditions to 10 kb: some implications for the origin of peraluminous melts from mafic rocks: Journal of Petrology, v. 27, p. 91–121.

Field, M. T., ms, 1975, Bedrock geology of the Ware area, central Massachusetts: Ph.D. thesis, Department of Geology and Geography, Contribution 22, University of Massachusetts, Amherst, 186 p.

Gill, J. B., and Stork, A. L., 1979, Miocene low-K dacites and trondhjemites of Fiji, *in* Barker, Fred, editor, Trondhjemites, Dacites, and Related Rocks: New York, Elsevier Scientific Publishing Co., p. 629–649.

Green, T. H., and Pearson, N. J., 1986, Ti-rich accessory phase saturation in hydrous mafic-felsic compositions at high P, T: Chemical Geology, v. 54, p. 185–201.

Grove, T. L., and Kinzler, R. J., 1986, Petrogenesis of andesites, *in* Wetherill, G. W., Albee, A. L., and Stehli, F. G., editors, Annual Review of Earth and Planetary Sciences, v. 14: Palo Alto, Annual Reviews, Inc., p. 417–454.

Hacker, B. R., 1990, Amphibolite-facies-to-granulite-facies reactions in experimentally deformed, unpowdered amphibolite: American Mineralogist, v. 75, p. 1349–1361.

Hall, L. M., and Robinson, Peter, 1982, Stratigraphic-tectonic subdivisions of southern New England, *in* St. Julian, P., and Beland, J., editors, Major Structural Zones and Faults of the Northern Appalachians: Geological Association of Canada Special Paper 24, p. 14–41.

Hart, S. R., and Davis, K. E., 1978, Nickel partitioning between olivine and silicate melt: Earth and Planetary Science Letters, v. 40, p. 203–219.

Hawkins, J. W. Jr., 1977, Petrologic and geochemical characteristics of marginal basin basalts, *in* Talwani, Manik, and Pitman III, W. C., editors, Island Arcs, Deep Sea Trenches and Back Arc Basins: Washington, D.C., American Geophysical Union, p. 355–365.

Hawkins, J. W., Bloomer, S. H., Evans, C. A., and Melchior, J. T., 1984, Evolution of intra-oceanic arc-trench systems: Tectonophysics, v. 102, p. 175–205.

Hawkins, J. W., and Melchior, J. T., 1985, Petrology of Mariana Trough and Lau Basin basalts: Journal of Geophysical Research, v. 90, no. B13, pl 11,431–11,468.

Helz, R. T., 1976, Phase relations of basalts in their melting ranges at P_{H2O} = 5 kbar. Part II. Melt compositions: Journal of Petrology, v. 17, p. 139–193.

Hildreth, Wes, 1981, Gradients in silicic magma chambers: implications for lithospheric magmatism: Journal of Geophysical Research, v. 86, no. B11, p. 10153–10192.

Hoffman, A. W., 1988, Chemical differentiation of the Earth: the relationship between mantle, continental crust, and oceanic crust: Earth and Planetary Science Letters, v. 90, p. 297–314.

Hollocher, Kurt, 1985, Characterization of pre-metamorphic alteration processes in mafic volcanics of the Middle Ordovician Partridge Formation, west-central Massachusetts: Geological Society of America Abstracts with Programs, v. 17, p. 25.

———— ms, 1985, Geochemistry of Metamorphosed volcanic rocks in the Middle Ordovician Partridge Formation, and amphibole dehydration reactions in the high-grade metamorphic zones of central Massachusetts: Ph.D. thesis, Department of Geology and Geography, Contribution 56, University of Massachusetts, Amherst, 275 p.

———— 1988, Geochemical comparisons of the Monson Gneiss and associated tonalitic Acadian plutons and overlying Ordovician volcanics, Massachusetts: Geological Society of America Abstracts with Programs, v. 20, p. 28.

———— 1991, Prograde amphibole dehydration reactions during high-grade regional metamorphism, central Massachusetts, U.S.A.: American Mineralogist, v. 76, p. 956–970.

Hollocher, Kurt, and Lent, Andrew, 1987, Comparative petrology of amphibolites in the Monson Gneiss and the Ammonoosuc and Partridge Volcanics, Massachusetts: Northeastern Geology, v. 9, p. 145–152.

Ikeda, Yasuo, and Yuasa, Makoto, 1989, Volcanism in nascent back-arc basins behind the Shichito Ridge and adjacent areas in the Izu-Ogasawara arc, northwest Pacific: evidence for mixing between E-type MORB and island arc magmas at the initiation of back-arc rifting: Contributions to Mineralogy and Petrology, v. 101, p. 377–393.

Irvine, T. N., and Baragar, W. R. A., 1971, A guide to the chemical classification of the common volcanic rocks: Canadian Journal of Earth Sciences, v. 8, p. 523–548.

Irving, A. J., 1978, A review of experimental studies of crystal/liquid trace element partitioning: Geochimica et Cosmochimica Acta, v. 42, p. 743–770.

Johnson, R. W., and Arculus, R. J., 1978, Volcanic rocks of the Witu islands, Papua New Guinea: the origin of magmas above the deepest part of the New Britain Benioff zone: Bulletin Volcanologique, v. 41, p. 609–655.

Kohn, M. J., 1991, Petrologic investigation of basement-cover relations in the Bronson Hill anticlinorium of southwestern New Hampshire: evidence for a major structural discontinuity: Geological Society of America Abstracts with Programs, v. 23, p. 54.

Laird, J., and Albee, A. L., 1981, High-pressure metamorphism in mafic schist from northern Vermont: American Journal of Science, v. 281, p. 97–126.

Langmuir, C. H., Bender, J. F., Bence, A. E., and Hanson, G. F., 1977, Petrogenesis of basalts from the FAMOUS area: mid-Atlantic ridge: Earth and Planetary Science Letters, v. 36, p. 133–156.

LeBas, M. J., LeMaitre, R. W., Streckeisen, A., and Zanettin, B., 1986, A chemical classification of volcanic rocks based on the total alkali-silica diagram: Journal of Petrology, v. 27, p. 745–750.

Leo, G. W., 1985, Trondhjemite and metamorphosed quartz keratophyre tuff of the Ammonoosuc Volcanics (Ordovician), western New Hampshire and adjacent Vermont and Massachusetts: Geological Society of America Bulletin, v. 96, p. 1493–1507.

———— 1991, Oliverian domes, related plutonic rocks, and mantling Ammonoosuc Volcanics of the Bronson Hill anticlinorium, New England Appalachians: U.S. Geological Survey, Professional Paper 1516, 92 p.

Leo, G. W., Zartman, R. E., and Brookins, D. G., 1984, Glastonbury Gneiss and mantling rocks (a modified Oliverian dome) in south-central Massachusetts and north-central Connecticut: geochemistry, petrogenesis, and isotopic age: U.S. Geological Survey, Professional Paper 1295, 47 p.

Longhi, John, 1991, Comparative liquidus equilibria of hypersthene-normative basalts at low pressure: American Mineralogist, v. 76, p. 785–800.

Lowder, G. G., and Carmichael, I. S. E., 1970, The volcanoes and caldera of Talasea, New Britain: geology and petrology: Geological Society of America Bulletin, v. 81, p. 17–38.

Maaløe, S., 1981, Magma accumulation in the ascending mantle: Journal of the Geological Society of London, v. 138, p. 223–236.

Mahood, G. A., 1981, A summary of the geology and petrology of the Sierra La Primavera, Jalisco, Mexico: Journal of Geophysical Research, v. 86, no. B11, p. 10137–10152.

Marcelot, G., Dupuy, C., Girod, M., and Maury, R. C., 1983, Petrology of Futuna Island lavas (New Hebrides): an example of calc-alkaline magmatism associated with the initial stages of back-arc spreading: Chemical Geology, v. 38, p. 23–37.

McKenzie, Dan, 1984, The generation and compaction of partially molten rock: Journal of Petrology, v. 25, p. 713–765.

McKenzie, Dan, and Bickle, M. J., 1988, The volume and composition of melt generated by extension of the lithosphere: Journal of Petrology, v. 29, p. 625–679.

Meijer, A., 1983, The origin of low-K rhyolites from the Mariana frontal arc: Contributions to Mineralogy and Petrology, v. 83, p. 45–51.

Merzbacher, Celia, and Eggler, D. H., 1984, A magmatic geohygrometer: application to Mount St. Helens and other dacitic magmas: Geology, v. 12, p. 587–590.

Meschede, 1986, A method of discriminating between different types of mid-ocean ridge basalts and continental tholeiites with the Nb-Zr-Y diagram: Chemical Geology, v. 56, p. 207–218.

Miyashiro, Akiho, and Shido, Fumiko, 1975, Tholeiitic and calc-alkaline series in relation to the behaviors of titanium, vanadium, chromium, and nickel: American Journal of Science, v. 275, p. 265–277.

Mullen, E. D., 1983, $MnO/TiO_2/P_2O_5$: a minor element discriminant for basaltic rocks of oceanic environments and its implications for petrogenesis: Earth and Planetary Science Letters, v. 62, p. 53–62.

Mutschler, F. E., Rougon, K. J., Lavin, O. P., and Huges, R. D., 1981, PETROS—a data bank of major element chemical analyses of igneous rocks for research and teaching: Version 6.1: Boulder, Colorado, National Oceanographic and Atmospheric Administration, National Geophysical and Solar-terrestrial data center.

Noble, D. C., Vogel, T. A., Peterson, P. S., Landis, G. P., Grant, N. K., Jezek, P. A., and McKee, E. H., 1984, Rare-element-enriched, S-type ash-flow tuffs containing phenocrysts of muscovite, andalusite, and sillimanite, southeastern Peru: Geology, v. 12, p. 35–39.

Nye, C. J., and Reid, M. R., 1986, Geochemistry of primary and least fractionated lavas from Okmok volcano, central Aleutians: implications for arc magmagenesis: Journal of Geophysical Research, v. 91, no. B10, p. 10271–10287.

Pearce, J. A., 1976, Statistical analysis of major element patterns in basalts: Journal of Petrology, v. 17, p. 15–37.

———— 1980, Geochemical evidence for the genesis and eruptive setting of lavas from Tethyan ophiolites, *in* Panayiotou, A., editor, Ophiolites: Geological Survey Department of Cyprus, p. 261–272.

———— 1983, Role of the sub-continental lithosphere in magma genesis at active continental margins, *in* Hawkesworth, C. J., and Norry, M. J., editors, Continental Basalts and Mantle Xenoliths, Cheshire, United Kingdom, Shiva Publishing Co, p. 230–250.

Pearce, J. A., and Cann, J. R., 1973, Tectonic setting of basic volcanic rocks determined using trace element analyses: Earth and Planetary Science Letters, v. 19, p. 290–300.

Pearce, J. A., Harris, N. B. W., and Tindle, A. G., 1984, Trace element discrimination diagrams for the tectonic interpretation of granitic rocks: Journal of Petrology, v. 25, p. 956–983.

Pearce, J. A., and Norry, M. J., 1979, Petrogenetic implications of Ti, Zr, Y, and Nb. Variations in volcanic rocks: Contributions to Mineralogy and Petrology, v. 69, p. 33–37.

Pickering, K. T., 1987, Deep-marine foreland basin and forearc sedimentation: a comparative study from the Lower Paleozoic Northern Appalachians, Quebec and Newfoundland, *in* Lettert, J. K., and Zuffa, G. G., editors, Marine Clastic Sedimentology: Boston, Graham and Trotman, p. 190–211.

Purman, G. W., and Alfors, J. T., 1969, Geochemistry and petrology of the Rocky Hill stock, Tulare County, California: Geological Society of America Special Paper 120, 109 p.

Reagan, M. K., and Meijer, Arend, 1984, Geology and geochemistry of early arc-volcanic rocks from Guam: Geological Society of America Bulletin, v. 95, p. 701–713.

Robinson, Peter, and Hall, Leo, 1980, Tectonic synthesis of southern New England, *in* Wones, D. R., editor, The Caledonides in the U.S.A., Symposium on IGCP Project 27, Caledonide orogen: Blacksburg, Virginia, Virginia Polytechnic Institute and State University, p. 73–82.

Robinson, Peter, Tracy, R. J., Hollocher, Kurt, Berry, H. N. IV, and Thomson, J. A., 1989, Basement and cover in the Acadian metamorphic high of central Massachusetts, *in* Chamberlain, C. P., and Robinson, Peter, editors, Styles of Acadian Metamorphism with Depth in the Central Acadian High, New England: University of Massachusetts, Amherst, Department of Geology and Geography, Contribution 63, p. 69–140.

Robinson, P. T., Brem, G. F., and McKee, E. H., 1984, John Day Formation of Oregon: a distal record of early Cascade volcanism: Geology, v. 12, p. 229–232.

Robinson, Peter, Tucker, R. D., and Hollocher, Kurt, 1989, The nature of the Bronson Hill zone during the Taconian Orogeny (abstract), *in* Colpron, M., and Doolan, B., editors, Quebec-Vermont Appalachian Workshop Proceedings: Burlington, Vermont, University of Vermont, p. 26–28.

Roeder, P. S., and Emslie, R. F., 1970, Olivine-liquid equilibrium: Contributions to Mineralogy and Petrology, v. 29, p. 275–289.

Ryerson, F. J., and Watson, E. B., 1987, Rutile saturation in magmas: implications for Ti-Nb-Ta depletion in island-arc basalts: Earth and Planetary Science Letters, v. 86, p. 225–239.

Schumacher, J. C., ms, 1983, Stratigraphic, geochemical, and petrologic studies of the Ammonoosuc Volcanics, north-central Massachusetts and southwestern New Hampshire: Ph.D. thesis, Department of Geology and Geography, University of Massachusetts, Amherst, 237 p.

———— 1988, Stratigraphy and geochemistry of the Ammonoosuc Volcanics, central Massachusetts and southwestern New Hampshire: American Journal of Science, v. 288, p. 619–663.

Shervais, J. W., 1982, Ti-V plots and the petrogenesis of modern and ophiolitic lavas: Earth and Planetary Science Letters, v. 59, p. 101–118.

Shumway, D. O., ms, 1984, Geochemistry of the Ammonoosuc Volcanics: tectonic setting of massive sulfide ore deposits: M.S. thesis, Department of Geology, Dartmouth College, 102 p.

Smith, I. E. M., and Johnson, R. W., 1981, Contrasting rhyolite suites in the late Cenozoic of Papua New Guinea: Journal of Geophysical Research, v. 86, no. B11, p. 10257–10272.

Spulber, S. D., and Rutherford, M. J., 1983, The origin of rhyolite and plagiogranite in oceanic crust: an experimental study: Journal of Petrology, v. 24, p. 1–25.

Stanley, R. S., and Ratcliffe, N. M., 1985, Tectonic synthesis of the Taconian Orogeny in western New England: Geological Society of America Bulletin, v. 96, p. 1227–1250.

Stern, R. J., Lin, Ping-Nan, Morris, J. D., Jackson, M. C., Fryer, Patricia, Bloomer, S. H., and Ito, Emi, 1990, Enriched back-arc basin basalts from the northern Mariana Trough: implications for the magmatic evolution of back-arc basins: Earth and Planetary Science Letters, v. 100, p. 210–225.

Streckeisen, A., 1967, Classification and nomenclature of igneous rocks: Nues Jahrbuch für Mineralogie Abhandlungen, v. 107, p. 144–240.
Sun, S. S., 1980, Lead isotopic study of young volcanic rocks from mid-ocean ridges, ocean islands and island arcs: Philosophical Transactions of the Royal Society of London, v. A297, p. 409–445.
Swanson, E. R., and McDowell, F. W., 1985, Geology and geochronology of the Tomochic caldara, Chihuahua, Mexico: Geological Society of America Bulletin, v. 96, p. 1477–1482.
Tarney, John, Saunders, A. D., and Weaver, S. D., 1977, Geochemistry of volcanic rocks from the island arcs and marginal basins of the Scotia arc region, *in* Talwani, Manik, and Pitman III, W. C., editors, Island Arcs, Deep Sea Trenches, and Back Arc Basins: Washington, D. C., American Geophysical Union, p. 367–377.
Tatsumi, Yoshiyuki, 1983, Generation of arc basalt magmas and thermal structure of the mantle wedge in subduction zones: Journal of Geophysical Research, v. 88, no. B7, p. 5815–5825.
Tatsumi, Yoshiyuki, and Koyaguchi, Takehiro, 1989, An absarokite from a phlogopite lherzolite source: Contributions to Mineralogy and Petrology, v. 102, p. 34–40.
Thompson, P. J., ms, 1985, Stratigraphy, structure, and metamorphism in the Monadnock Quadrangle, New Hampshire: Ph.D. thesis, Department of Geology and Geography, Contribution 58, University of Massachusetts, Amherst, 191 p.
Thompson, R. N., Morrison, M. A., Hendry, G. L., and Parry, S. J., 1984, An assessment of the relative roles of crust and mantle in magma genesis: an elemental approach: Royal Society of London Philosophical Transactions, v. A310, p. 549–590.
Toksöz, M. N., and Hsui, A. T., 1978, Numerical studies of back-arc convection and the formation of marginal basins: Tectonophysics, v. 50, p. 177–196.
Tracy, R. J., Robinson, Peter, and Thompson, A. B., 1976, Garnet composition and zoning in the determination of temperature and pressure of metamorphism, central Massachusetts: American Mineralogist, v. 61, p. 762–775.
Tracy, R. J., Robinson, Peter, and Wolff, R. A., 1984, Metamorphosed ultramafic rocks in the Bronson Hill anticlinorium, central Massachusetts: American Journal of Science, v. 284, p. 530–558.
Tucker, R. D., and Robinson, Peter, 1990, Age and setting of the Bronson Hill magmatic arc: A re-evaluation based on U-Pb zircon ages in southern New England: Geological Society of America Bulletin, v. 102, p. 1404–1419.
Uyeda, Seiya, 1977, Some basic problems in the trench-arc-back arc system, *in* Talwani, Manik, and Pitman III, W. C., editors, Island Arcs, Deep Sea Trenches and Back Arc Basins: Washington, D.C., American Geophysical Union, p. 1–14.
Vennum, W. R., and Rowley, P. D., 1986, Reconnaissance geochemistry of the Lassiter Coast intrusive suite, southern Antarctic peninsula: Geological Society of America Bulletin, v. 97, p. 1521–1533.
Watson, E. B., 1979, Apatite saturation in basic to intermediate magmas: Geophysical Research Letters, v. 6, p. 937–940.
Weaver, S. D., Saunders, A. D., Pankhurst, R. J., and Tarney, John, 1979, A geochemical study of magmatism associated with the initial stages of back-arc spreading: Contributions to Mineralogy and Petrology, v. 68, p. 151–169.
Winchester, J. A., and Floyd, P. A., 1977, Geochemical discrimination of different magma series and their differentiation products using immobile elements: Chemical Geology, v. 20, p. 325–343.
Winkler, H. G. F., 1979, Petrogenesis of Metamorphic Rocks, 5th edition: New York, Springer Verlag Publishing Co., 347 p.
Wolff, R. A., ms, 1978, Ultramafic lenses in the Middle Ordovician Partridge Formation, Bronson Hill anticlinorium, central Massachusetts: M.S. thesis, Department of Geology and Geography, Contribution 34, University of Massachusetts, Amherst, 162 p.
Wood, D. A., 1979, Dynamic partial melting: its application to the petrogenesis of basalts erupted in Iceland, the Faeroe Islands, the Isle of Skye (Scotland) and the Troodos massif (Cyprus): Geochimica et Cosmochimica Acta, v. 43, p. 1031–1046.
———— 1980, The application of a Th-Hf-Ta diagram to problems of tectonomagmatic classification and to establishing the nature of crustal contamination of basaltic lavas on the British Tertiary Volcanic Province: Earth and Planetary Science Letters, v. 50, p. 11–30.
Zartman, R. E., and Leo, G. W., 1985, New radiometric ages on gneisses of the Oliverian domes in New Hampshire and Massachusetts: American Journal of Science, v. 285, p. 267–280.
Zen, E-An, editor, 1983, Bedrock Geologic Map of Massachusetts, 1:250,000: U.S. Geological Survey, 3 sheets.